Award Number: DAMD17-01-1-0788

TITLE: DU Fragment Carcinogenicity: Extrapolation of Findings in Rodents to Man

PRINCIPAL INVESTIGATOR: Fletcher F. Hahn, Ph.D.

CONTRACTING ORGANIZATION: Lovelace Biomedical and Environmental Research Institute
Albuquerque, NM 87108

REPORT DATE: March 2004

TYPE OF REPORT: Final

PREPARED FOR: U.S. Army Medical Research and Materiel Command
Fort Detrick, Maryland 21702-5012

DISTRIBUTION STATEMENT: Approved for Public Release;
Distribution Unlimited

The views, opinions and/or findings contained in this report are those of the author(s) and should not be construed as an official Department of the Army position, policy or decision unless so designated by other documentation.

REPORT DOCUMENTATION PAGE

Form Approved
OMB No. 074-0188

1. AGENCY USE ONLY (Leave blank)	2. REPORT DATE	3. REPORT TYPE AND DATES COVERED
	March 2004	Final (1 Sep 2001 - 29 Feb 2004)

4. TITLE AND SUBTITLE

DU Fragment Carcinogenicity: Extrapolation of Findings in Rodents to Man

5. FUNDING NUMBERS

DAMD17-01-1-0788

6. AUTHOR(S)

Fletcher F. Hahn, Ph.D.

7. PERFORMING ORGANIZATION NAME(S) AND ADDRESS(ES)

Lovelace Biomedical and Environmental
Research Institute
Albuquerque, NM 87108

E-Mail: fhahn@lrri.org

8. PERFORMING ORGANIZATION REPORT NUMBER

9. SPONSORING / MONITORING AGENCY NAME(S) AND ADDRESS(ES)

U.S. Army Medical Research and Materiel Command
Fort Detrick, Maryland 21702-5012

10. SPONSORING / MONITORING AGENCY REPORT NUMBER

11. SUPPLEMENTARY NOTES

12a. DISTRIBUTION / AVAILABILITY STATEMENT

Approved for Public Release; Distribution Unlimited

12b. DISTRIBUTION CODE

13. ABSTRACT (Maximum 200 Words)

Rats with implants of DU or injections of Thorotrast® in muscles developed soft tissue sarcomas (STS). Tissue samples from this previously conducted life-span study were used to determine certain molecular changes associated with the STS induction. Significantly increased p53 expression was present in DU-induced STS compared with those induced by Thorotrast®. However, p53 expression was not found in the few microscopic tumors of the capsules around the implants or in benign tumors. Expression of the oncogenes MDM2, c-myc, and p21 was low and not related to DU or Thorotrast®. The oncogene K-ras was not mutated in any tumors. The pattern of differential gene expression in the DU-induced STS was not similar to the Thorotrast®-induced STS. Few expressed genes were similar and many were exclusively expressed. These findings suggest that the mechanism of carcinogenesis is not the same for DU and Thorotrast®-induced STS.

Histologic study of the embedded DU showed that the DU rapidly corrodes in muscle. In 7 days corrosion, and the acute tissue reaction to it, was visualized in radiographs of the tissues. Corrosion continued causing an enlargement of the embedded DU on radiographs. This information may be useful in interpreting radiographs of DU embedded in humans.

14. SUBJECT TERMS

Depleted uranium (DU), carcinogenesis, rodents, molecular changes

15. NUMBER OF PAGES

59

16. PRICE CODE

17. SECURITY CLASSIFICATION OF REPORT	18. SECURITY CLASSIFICATION OF THIS PAGE	19. SECURITY CLASSIFICATION OF ABSTRACT	20. LIMITATION OF ABSTRACT
Unclassified	Unclassified	Unclassified	Unlimited

TABLE OF CONTENTS

I. INTRODUCTION

A. Background

A small number of Gulf War veterans had fragments of depleted uranium alloyed with 0.75% titanium (DU) embedded in their muscles and soft tissues. The large number, small size, or inaccessibility of the fragments made surgical removal difficult. Thirty-three of these survivors are being followed medically to detect any untoward health effects (McDiarmid *et al.*, 2000, 2004). Some of these veterans had elevated concentrations of uranium in the urine 10 years after wounding. The persistence of these elevated urine concentrations indicates an ongoing mobilization of uranium from the embedded fragments, which results in a chronic systemic exposure. Thus, DU fragments are not inert foreign bodies in the soft tissues and may react differently in the body compared with other embedded shrapnel.

A life-span study conducted at LRRI has shown that DU is carcinogenic in rats (Hahn *et al.*, 2002). The study was designed to determine carcinogenicity of DU and compare the carcinogenicity to that of a non-radioactive metal tantalum (Ta), as a negative control, and to injections of Thorotrast® (a colloid of radioactive thorium dioxide) as a positive control. DU, in four squares (2.5 × 2.5 × 1.5 mm or 5.0 × 5.0 × 1.5 mm) or pellets (2.0 × 1.0 mm diameter), was surgically implanted in the thigh muscles of male Wistar rats, 50 rats per treatment group. Ta (5.0 × 5.0 × 1.0 mm) was similarly implanted.

At the time of death, the implants of DU or Ta were encapsulated with connective tissue. Injected Thorotrast® did not induce capsule formation, but localized in and around the muscles at the injection site.

Soft tissue tumors of various types were associated with many of the implants (Table 1). The most commonly found tumors were malignant fibrous histiocytomas and fibrosarcomas. The three osteosarcomas noted were of soft tissue origin and not associated with the skeleton. Although there was a higher number of fibrosarcomas in the Thorotrast®-treated rats and a broader range of tumors in the DU-treated rats, no specific tumor type could be attributed to a specific treatment. The incidence of the tumors was increased in the rats with the largest DU implants when compared with the sham or negative (Ta) controls (Figure 1). The difference was significant ($p \leq 0.023$) using a Fisher's exact test. The Thorotrast® (positive control) animals had

a significant increase in soft tissue tumors over the number in DU-implanted rats. In addition, there was a fragment size-related response in the DU-treated rats.

Table 1
Implant-Associated Soft Tissue Tumor Types

	Depleted Uranium	Thorotrast®	Tantalum	Surgical Control
Benign fibrous histiocytoma	1	0	0	0
Fibroma	1[a]	0	0	0
Granular cell myoblastoma	0	1	0	0
Malignant fibrous histiocytoma	7[a]	13	2	0
Fibrosarcoma	2	10	0	0
Osteosarcoma	2	1	0	0

[a]One rat had two tumors.

The tumor response with DU could not be explained by physical surface area alone because the response with the Ta implants of similar size was much lower. There was, however, a correlation with the initial surface alpha radioactivity. This initial activity was calculated from the physical characteristics of the DU fragments and the Thorotrast® colloid. The calculated radiation dose rate from DU, averaged over a 50-μm tissue thickness surrounding the implant, was 0.004 Gy/day. Calculation of an alpha dose from injected Thorotrast® was more complicated because of the complex thorium decay series of radioisotopes and the semi-liquid nature of Thorotrast®. To calculate the dose rate soon after injection, a sphere with the volume of 0.025 cm^3 was assumed. The dose rate was calculated as 0.011 Gy/day. Radiographs showed that the physical shape of both the fragments and the colloid changed within 21 days after implantation. Thus, the surface alpha radioactivity changed with time as the shape of the implants changed. The accumulation of the Thorotrast® in macrophages probably increased the surface alpha activity with time, as did the fragmentation of the DU.

These findings clearly indicate that DU fragments of sufficient size or surface area are carcinogenic in rats. Whether or not they are carcinogenic for man is not clear. The mechanism by which DU induces tumors has importance in extrapolation of these findings from rats to man. If DU is considered to induce tumors by a foreign-body mechanism, then soft tissue tumor incidence for foreign bodies should be used in extrapolations. If a radiation mechanism

predominates, then soft tissue tumor incidence for radioactive compounds, such as Thorotrast®, should be used for extrapolations. If yet another mechanism is involved, other tumor incidence data should be used in extrapolation.

Based on the evidence in hand, DU probably does not induce tumors in rats solely by a foreign-body mechanism. It may induce tumors by a radiation mechanism, however, or some less-defined irritant response. Determining the most likely mechanism would aid in extrapolation of the evidence for DU carcinogenicity to man. Materials carcinogenic in rats are frequently, but not always, carcinogenic in man. Exceptions may occur when the mechanism of carcinogenesis in rats is not operative in man (MacDonald and Scribner, 1999).

Two approaches were taken to clarify if soft tissue tumors are likely to be induced in man by embedded DU fragments. We examined tissues from tumors induced by implanted DU fragments and by injected Thorotrast®, a radioactive compound, to determine if gene changes commonly associated with soft tissue tumors in man are expressed. The specific gene changes examined were the expression of p53, MDM2, p21 and c-myc, and mutation of K-ras. Four genes were selected as potential biomarkers based on a preliminary study and review of the literature.

p53 – p53 was chosen because of its relatively high frequency of mutation in human soft tissue sarcomas and in rodent soft tissue sarcomas induced with materials placed subcutaneously. In humans, the frequency of p53 aberrant levels of protein detected by immunohistochemical staining is 43% with a range in different studies from 6 to 70% (Mousses *et al.*, 1996; Taubert *et al.*, 1995, 1998; Yoo *et al.*, 1997; Soini *et al.*, 1992; Wadayama *et al.*, 1993). This is usually indicative of mutation. In one study of radiation-induced soft tissue sarcomas, 9 of 11 sarcomas were positive for p53, an indication of p53 dysfunction (Taubert *et al.*, 1998). In rats, one study showed 14 of 70 soft tissue sarcomas positive for p53 by immunohistochemical staining (Stefanou *et al.*, 1998). A study of mandibular irradiation in rabbits demonstrated p53 staining in 10 of 17 osteosarcomas (Buchholz *et al.*, 1999). p53 mutations also occur in radiation-induced mammary cancer in mice (Selvanayagam *et al.*, 1995) and in Thorotrast®-induced liver cancers in man (Kamikawa *et al.*, 1999). In both the radiation studies, however, p53 was mutated late in the carcinogenic process, and probably not affected by direct radiation damage.

MDM2 – The regulation of cell growth by p53 depends on activating transcription of MDM2 by p53 (Momand *et al.*, 1992). Overexpression of the MDM2 gene interferes with

transcriptional activation of wild-type p53, thereby abrogating normal p53 function. In addition to this close correlation, several studies of human soft tissue sarcomas have reported the overexpression of MDM2 (Cordon-Cardo *et al.*, 1994; Leach *et al.*, 1993; Reid *et al.*, 1996; Molina *et al.*, 1999; Szadowska *et al.*, 1999). The average percentage of tumors positive for MDM2 was about 26% with a range from 9.7 to 48%. We are unaware of any studies done on the soft tissue sarcomas of rodents. However, transgenic, MDM2 null, mice have been used to study the interaction between MDM2 and p53 *in vivo* indicating that the molecular mechanism is operative in rodents (McDonnell *et al.*, 1999).

p21 – This protein is important in regulation of the cell cycle and falls in the p53 activation pathway. p53 blocks progression through the cell cycle by activating the transcription of p21, which in turn, inhibits the activity of a number of cyclin-CDK complexes that modulate the cell cycle.

c-myc – This oncogene was selected based on evidence from both humans and rodents. One study in man showed marked c-myc amplifications in 7 of 23 soft tissue sarcomas (Barrios *et al.*, 1994), and another showed amplifications in 8 of 43 sarcomas (Castresana *et al.*, 1994). In mice, c-myc was also amplified in soft tissue sarcomas induced by plastics, methyl cholanthrene, or tocopherol in the subcutis (Kuwashima *et al.*, 1993, Niwa *et al.*, 1989). In contrast, none of eight radiation-induced sarcomas of the subcutis had c-myc amplifications (Niwa *et al.*, 1989). This finding indicates that c-myc expression may be an aid in separating the radiation-induction mechanism from other mechanisms of cancer induction.

K-ras – Studies with DU suggest that K-ras may be important in carcinogenesis. *In vitro* studies have shown that DU causes transformation of human osteoblasts and expression of high levels of K-ras by these cells (Miller *et al.*, 1998b). In rats, pellets of DU embedded in the muscles caused increased levels of K-ras in the muscles (Miller, 1988). Tumors induced by BAP injected in to the subcutis of rats also had K-ras mutations (5/70) as determined by immunohistochemical staining (Stefanou *et al.*, 1998). However, only one report was found concerning ras mutations in human soft tissue sarcomas. Point mutations in H-ras were found in two of six malignant fibrous histiocytomas (Wilke *et al.*, 1993).

In addition, we used a differential gene expression analysis to identify novel genes in DU-induced tumors and to compare them with genes expressed in Thorotrast®-induced tumors. A similarity of gene expression patterns may help identify the mechanism of carcinogenesis of

DU-induced tumors in rats. cDNA microarrays are available to simultaneously identify gene expression from multiple genes. Some of these genes may serve as biomarkers for soft tissue sarcomas and their precursor lesions. Hybridization to cDNA microarrays allowed the simultaneous parallel expression analysis of multiple genes. This technique has been used successfully to investigate gene expression profiles in a group of cell lines from alveolar rhabdomyosarcomas, a type of soft tissue sarcoma of children (Khan *et al.*, 1998). Expression profiles indicate similarities and differences in gene expression between two samples. Similarity of gene patterns would suggest a similarity in the mechanism of carcinogenesis and difference in gene patterns would suggest a difference in the mechanism of carcinogenesis. In addition, candidates for molecular biomarkers might also be identified.

Another approach to determine how the finding of tumors in rats should be extrapolated to man is to study the similarity of the tissue reactions in several species of animals (Huff, 1999). Since the latent period for cancer is related to normal life span, it is impractical to observe longer-lived species until tumors occur. However, if the early reactions to DU are similar in several species, extrapolation of the cancer findings to man is more certain. More recently, molecular biomarkers of neoplasia have been shown to occur in the tissues before frank neoplasms are observed (Belinsky *et al.*, 1998; Dong *et al.*, 2001). Thus, any molecular biomarkers found in the rat tissue capsules before the onset of tumors may also be present in other species. In addition, any such biomarkers could be sought in any tissue that may become available from veterans wounded with DU shrapnel (McDiarmid *et al.*, 2000, 2004).

B. Purpose

This project focused on identifying molecular biomarkers of neoplasia in the connective tissue capsules and neoplasms around DU implanted in rats. The results set the stage for using these markers in other species, including man, to evaluate the carcinogenicity of DU in humans. In addition, we compared the appearance of these markers and the expression of genes in DU- and Thorotrast®-induced tumors to help determine if DU induces tumors by a radiation-dependent mechanism.

Three hypotheses were tested:

1. Patterns of gene expression in soft tissue sarcomas associated with implanted DU differ from the patterns in sarcomas induced by injected Thorotrast®.

2. The specific oncogenes and tumor suppressor genes in soft tissue sarcomas associated with implanted DU will be expressed in the capsules that surround DU and are antecedent lesions to the sarcomas.

3. Novel tumor genes expressed in the soft tissue sarcomas associated with implanted DU and injected Thorotrast® will be expressed in the capsules that surround DU and are precursor lesions to the sarcomas.

C. Statement of Work

The original Statement of Work was modified subsequent to the peer review of the project on December 5–6, 2002, organized by the American Institute of Biological Sciences.

1. Objective 1 – Determine presence of selected molecular biomarkers of neoplasia (p53, MDM2, p21, c-myc, K-ras) in DU- and Thorotrast®-induced tumors.

2. Objective 2 – Apply molecular biomarkers of neoplasia to the microscopic tumors and capsule samples to determine potential early biomarkers of DU-induced tumors.

3. Objective 3 – Compare patterns of gene expression related to DU- and Thorotrast®-induced sarcomas and to normal muscle.

4. Objective 4 – Correlate radiographic and morphologic tissues changes over time after implantation of DU.

5. Objective 5 – Further characterize the morphologic and molecular nature of the tumors.

II. BODY OF THE REPORT

A. Methods

1. Source Materials

The tissues examined were obtained from the carcinogenesis study of implanted DU or Tantalum (Ta), or injected Thorotrast® (Hahn *et al.*, 2002). Formalin-fixed tissues were placed in 10% neutral buffered formalin (NBF) and embedded in paraffin, usually within 4 days. The fixed soft tissue tumor tissues available from the 2-year bioassay study and serial sacrifice study are noted in Table 2.

Table 2
Source Materials: Implant-Induced Soft Tumor Tissues
Available from Carcinogenesis Study
(Fixed in 10% NBF)

	Rats	Gross Tumors	Microscopic Tumors	Capsules/ Muscle[a]
Sham	50	0	0	0
Ta	50	1	1	195
Thorotrast®	50	20	5	21
DU pellet	50	0	0	178
DU 2 × 2 mm	50	2	1	183
DU 5 × 5 mm	49	8	1	172

[a]Number of capsules for DU and Ta rats. Number of muscle injection sites for Thorotrast®.

In addition, tissues were available from a serial sacrifice study conducted in the earlier project (Table 3). These rats were implanted with the 2.5 × 2.5 mm fragments and sacrificed at various intervals out to 18 months after fragment implantation. Sham rats had the same surgical procedure performed, but no implant was inserted into the muscles.

Table 3
Source Materials: Implant-Related Tissues
Available from Serial Sacrifice Study
(Fixed in 10% NBF)

Time After Implant (Days)	Sham Site[a]	DU 2.5 × 2.5 Site[a]
0	4	0
7	0	4
30	0	4
60	0	4
124	0	4
182	4	4
275	0	4
365	5	5
550	3	4

[a]Number of rats with available tissues.

2. Immunohistochemical Analysis for Molecular Changes

p53: Analyses for overexpression of p53 protein were performed on 5-micra, paraffin-embedded tissue sections using techniques previously performed at the Institute (Belinsky *et al.*, 1996; Nickell-Brady *et al.*, 1994; Swafford *et al.*, 1995). Vectastain ABC immunoperoxidase reagents (Vector Laboratories, Burlingame, CA), detection chromogen 3,3'-diaminobenzidine tetrahydrochloride (Zymed Laboratories, Inc., S. San Francisco, CA), and the primary p53 polyclonal antibody CM1 (SigNet, Dedham, MA) were used. Negative control slides were reacted with normal rabbit serum. A sarcoma induced in nude mice injected subcutaneously with cells from an SV40-immortalized cell line served as a positive control. Staining reactions in the nucleus were graded 0 to 4 based on intensity and distribution of staining noted using light microscopy.

MDM2: Analyses for MDM2 expression were performed on tissue sections adjacent to those used for the p53 analyses using techniques previously performed at the Institute (Belinsky *et al.*, 1996; Swafford *et al.*, 1995). The primary antibody was a mouse monoclonal antibody SMP14 from ascites fluid (provided by S. M. Picksley). Biotinylated antimouse secondary antibody (BioGenex Link, BioGenex, San Ramon, CA), a strepavidin peroxidase system (BioGenex Peroxidase Conjugated Strepavidin Label), and the detection chromogen 3,3'-diaminobenzidine tetrahydrochloride (Zymed Laboratories, Inc.) were used to detect MDM2 protein. Negative control sections were reacted with mouse ascites fluid. Paraffin-embedded rat Clone-6 cells (provided by A. J. Levine) served as positive control for MDM2 immunoreactivity. These cells contain a mutated, temperature-sensitive p53 and over expressed MDM2 when incubated at 32°C. Staining reactions in the nucleus were graded 0 to 4 based on intensity and distribution of staining noted using light microscopy.

C-myc: Analyses for c-myc expression were performed using 5-micra, paraffin-embedded sections. Immunoperoxidase staining was performed using the Zymed Histomouse SP kit (Zymed Laboratories, Inc.). The primary antibody was a murine c-Myc IgG2a monoclonal antibody, non cross-reactive with n-Myc or l-Myc (Santa Cruz Biotechnology, Inc., Santa Cruz, CA). Sections were treated with biotinylated secondary antibody, then with avidin-biotin horseradish peroxidase. The detection chromogen was 3,3'-diaminobenzidine tetrahydrochloride (Zymed Laboratories, Inc.). Staining reactions in the

nucleus were graded 0 to 4 based on intensity and distribution of staining noted using light microscopy.

p21: Analyses for expression of p21 were preformed using 5-micra, paraffin-embedded sections. Antigen retrieval was performed by boiling the slides in a microwave for 10 min in 0.01 M citrate buffer, pH 6.0. The primary antibody was a murine monoclonal [anti-p21 (F-5) 1:50 dilution, Santa Cruz Biotechnology, Santa Cruz, CA]. Slides were rinsed in automation buffer (Biomeda, Foster City, CA) followed by incubation with biotinylated secondary antibody (Vector Laboratories, Burlingame, CA) After rinsing in automation buffer the sections were incubated in preformed avidin-biotin alkaline phosphatase complex solution (Vectastain Standard ABC-AP Kit, Vector Laboratories, Burlingame, CA). The sections were developed with Vector Red alkaline phosphatase substrate for (Vector Laboratories, Burlingame, CA). A human breast carcinoma, known positive for p21, was used as a positive control. Staining reactions in the nucleus were graded 0 to 4 based on intensity and distribution of staining noted using light microscopy.

3. Analyses of K-ras Codon 12 Mutations

DNA extraction: Slides, stained with hematoxylin and eosin, were used to locate the tumors for detection of K-ras mutations. High molecular weight DNA was isolated and amplified by polymerase chain reaction (PCR) as described by Levi *et al.* (1991). Tissue from paraffin-embedded tumors was isolated by microdissection of 10 slides cut at 10 μm thick. The tumor tissue was digested with Protease K, RNAse T1, and RNAse A (Sigma, St. Louis, MO) at 55°C overnight. DNA was extracted using standard phenol/chloroform/isoamyl alcohol techniques and ethanol precipitated. DNA was resuspended in TE buffer (10 mM Tris-HCl, 1 mM EDTA, pH 7.5) and quantified using a Beckman DU 640 spectrophotometer (Fullerton, CA). DNA from an A/J mouse lung tumor was used as a positive control for a K ras, codon 12 mutation.

Detection of K-ras mutations: A mutant codon 12 K-ras PCR enrichment restriction fragment length polymorphism (RFLP) analysis was used to detect K-ras mutations in the soft tissue tumors (Belinsky *et al.*, 1996, 1997; Nickell-Brady *et al.*, 1994). The assay relies on the construction of the K-ras 5′ first exon primer where the G residue at the first position of codon 11 is replaced with a C. Amplification of a wild-type K-ras allele using this primer

creates gene fragments harboring a *BstN*1 restriction enzyme cleavage site (CCTGG) overlapping the first two bases of codon 12. Amplification of a K-ras mutant at either the first or second position of codon 12 does not create gene fragments carrying this *BstN*1 restriction site. Following initial *BstN*1 cleavage, the remaining uncut mutant, K-ras codon 12-containing fragment, was selectively reamplified and redigested.

Duplicate symmetric amplifications of K-ras exon 1 were performed using 50 pmoles of the *BstN*1 restriction site creating primer K1E and 50 pmoles of primer K1B. The cycling pattern consisted of 94°C for 1 minute, 52°C for 1 minute, and 73°C for 30 seconds for 12 cycles. The PCR products were digested with the restriction endonuclease *BstN*1 using conditions recommended by the manufacturer (New England Biolabs, Beverly, MA). Following the restriction digestion, the samples were precipitated with ethanol; after resuspension, one-quarter of the samples were used as the template for a second selective PCR amplification of 26 cycles and was identical to the first pattern. The PCR products were digested a second time using the same technique. K-ras exon 1 restriction fragments were resolved by electrophoresis of the DNA fragments through an 8% non-denaturing polyacrylamide gel.

4. Protocol for Differential Gene Expression Arrays

Rat cDNA expression arrays were used to survey the differences in gene expression between DU-induced sarcomas and Thorotrast®-induced sarcomas and between these sarcomas and normal muscle tissue. The experimental design for the comparisons made and the specific rats used is shown in Table 4. The number of frozen tissues available constrained the number of parameters that could be examined. Gene expressions were compared among tumor types (fibrosarcoma vs. malignant fibrous histiocytoma) and carcinogenic compounds (DU vs. Thorotrast®). Pooled normal muscle from five rats was used as the control tissue in each array.

Tissue was homogenized in lysis buffer and total RNA was isolated using Atlas™ Pure Total Labeling System (ClonTech Laboratories, Palo Alto, CA) per manufacturer's recommendations. Total RNA was DNase I treated and the quality was assessed by gel electrophoresis and quantified by spectrophotometry. Biotinylated oligo dT was used to select poly A+ mRNA from total RNA (10 µg) and strepavidin-linked magnetic beads (Dynabeads) were used to isolate the mRNA. The mRNA was used in a primer-specific cDNA probe synthesis with ^{32}P dATP. Labeled cDNA was purified using Nucleospin® RNA II spin columns

(ClonTech) and specific activity of ^{32}P-labeled probes was measured by determining the total radioactivity with a Proscan QC 2000 (Bioscan, Inc., Washington, DC).

Table 4
Tissues for Differential Gene Expression

Normal[a] Muscle	Thorotrast® Fibrosarcoma	Thorotrast® MFH	DU MFH
C 037[b]	C 034 (a)[c]	C 037 (a)	F 089 (b)
C 040	C 048 (b)	C 046 (c)	L 095 (c)
C 046	I 041 (c)	C 042 (b)	R 093 (d)
I 042	I 050 (d)	I 051 (d)	R 094 (a)
I 051			

[a]Normal RNA was a pooled sample of normal muscle.
[b]Rat number
[c]An array hybridization set (a–d) included one sample from each column. In total 16 hybridizations were done.

Hybridizations were performed on Rat Toxicology 1.2 nylon arrays (ClonTech) consisting of 1,176 known rat genes. Genes included are many known to be involved with neoplasia, tumor suppressors, oncogenes, differentiation genes, cell cycle genes and growth factors, as well as stress genes, enzyme genes, etc. associated with toxic reactions. Identical quadruplicate membranes from the same lot were hybridized with the normal muscle control or experimental cDNA probes. This allowed for direct comparison of the expression profiles of the different mRNA populations. Table 4 shows the rat number for tumor tissue used in the hybridization sets (a–d) and rat numbers for the pooled normal skeletal muscle sample.

The extent of hybridization was detected by PhosphorImager analysis. AtlasImage 2.7 was used to quantify the hybridization signal from the tiff images. Global normalization was performed to account for hybridization efficiencies on each array before comparison with normal rat skeletal muscle. Each group (a–d, Table 4) was hybridized to an individual array, global normalization was applied to each array and comparisons were made to the normal rat skeletal muscle. Results from quadruplicate hybridizations were averaged and changes in gene expression either an increase or decrease, was scored as significant using a 95% confidence level. GeneSpring software was used to further analyze the array data. An intensity cutoff ($I > 10$) was assigned as significantly present based upon visual inspection of the tiff images. Invariant genes and insignificant changes ($p > 0.05$) in gene expression were removed

from analysis. Comparisons using Venn diagrams to elucidate similarities between tumor types and induction by DU or Thorotrast® were determined.

5. Histologic Techniques for Tumor Characterization

The 5 micra, paraffin-embedded tumor tissue sections were stained with hematoxylin and eosin for tissue detail, with Masson's trichrome stain for presence of elastic and collagen fibers and with PTAH for presence of muscle fibers. In addition, immunohistochemical techniques were used to detect vimentin in the tissues. After antigen retrieval by boiling the slides in a microwave and blocking nonspecific staining with horse serum, tissue sections were incubated with mouse monoclonal primary antibody (Anti-Vimentin clone V9, 1:100 dilution, Dako Cytomation, Carpentaria, CA). Slides were rinsed with automation buffer (Biomeda, Foster City, CA) followed by incubation with biotinylated secondary antibody (Vector Laboratories, Burlingame, CA). The sections were incubated in preformed avidin-biotin alkaline phosphatase complex solution (Vectastain Standard ABC-AP Kit, Vector Laboratories, Burlingame, CA) and developed with Vector Red alkaline phosphatase substrate for 30 min (Vector Laboratories, Burlingame, CA). A human breast carcinoma was used as a positive control. Staining reactions in the cytoplasm were graded 0 to 4 based on intensity and distribution of staining noted using light microscopy.

B. Results

1. Morphologic Characterization of Capsules and DU- and Thorotrast®-Induced Soft Tissue Tumors

Hypotheses 1 and 3 of the project note that lesions in the capsules surrounding the DU implants are the precursors of the soft tissue sarcomas. Thus, knowing the histologic changes surrounding the implants and the timing of the changes was important. Tissue reaction around the 2.5 × 2.5 mm DU implants was obvious at 7 days and continued through 18 months implantation (Table 5). Moderate numbers of neutrophils and a few macrophages were present surrounding the implants at 7 days after implantation (Figure 2). The inflammation was still prominent at 1 month. Neutrophils were essentially absent from 2 to 18 months, although macrophages were still present at these times (Figure 3). Fibroblasts and small amounts of collagen were present around the implants at 7 days. The amount of fibrosis slowly increased over time, forming a distinct capsule around the implant.

Table 5
Histologic Grading of Capsules Around DU Implants

	Sacrifice Rats								Life-span Rats		
Implant Size	2.5 × 2.5 mm								1 mm diam	2.5 × 2.5 mm	5 × 5 mm
Survival - Months	1/4	1	2	4	6	9	12	18			
Number of Rats	4	4	4	4	4	4	5	4	48	48	49
Grading											
Acute Inflammatory Cells	1.8	1.0	0	0	0	0	0	0.5	0.08	0.27	0.31
Chronic Inflammatory Cells	2.3	3.0	1.8	1.3	2.3	1.8	1.2	1.0	1.4	1.4	1.1
Fibrosis	1.3	1.3	1.5	2.0	2.0	2.3	1.6	1.5	1.8	2.1	2.5
Degeneration	1.0	2.5	2.0	1.8	1.8	1.5	0.75	0.75	1.2	1.0	1.9
Mineralization	0	0	0	0	0	0.5	0.25	0.25	1.0	0.63	0.92
Corrosion Particles	1.3	1.8	1.8	1.5	1.8	1.3	1.2	1.3	1.2	0.69	1.6
Corrosion Fragments	0	0	0	0	2.0	2.0	2.8	3.0	0.08	2.2	2.0
Microscopic Tumor in Capsule	0	0	0	0	0	0	0	0	0	2	1

Grading is an average based on a scale from minimal (1) to marked (4).

Degeneration, consisting of proteinaceous and necrotic debris from the wall of the capsule, was frequently found at the interface of the capsule and the implant. The intensity of the degeneration was greatest at 1 month after implantation and gradually waned by 18 months. Mineralization of the necrotic debris and of the capsules was noted at 9 months after implantation and persisted to 18 months.

Small, microscopic black particles of corroded DU were visible in the capsules as early as 7 days after implantation and continuing though 18 months after implantation (Figure 4). In addition, large black fragments or shards visible to the naked eye were found in the wall of the capsules starting at 6 months and increasing in amount through 18 months (Figure 5).

These findings indicate that corrosion of the DU and inflammation occurred as early as 7 days after implant (Figure 6). Inflammatory cell numbers around the DU implants decreased with time but were always present. In contrast, fibrosis around the implants, initially seen at 7 days after implantation, slowly increased with time. The degree of fibrosis was related to the size of the fragment and the degree of corrosion as indicated by the number of shards and particles of DU in the tissues (Figure 7).

Also noted in Table 5 is the low number of microscopic tumors found in the capsules, only 3 of the 97 capsules around the largest two sizes of implants. The finding does reinforce the hypothesis that the tumors around fragments arise in the capsules.

The capsules around the Ta implants in the rats held for life span were characterized by scant fibrosis with very little inflammation and no degeneration or mineralization. The capsule walls were <0.1 mm thick with a smooth inner surface. No shards or particles of corrosion were present (Figure 8).

Capsules were not present around the Thorotrast® in rats held for life span. The lesion was an accumulation of Thorotrast®-laden macrophages scattered between muscle fibers and in the loose connective tissues between muscles. The macrophages were filled with a tan, coarsely granular material. These macrophages were not associated with inflammatory cells or fibrosis. The relative lack of tissue reaction was striking when compared to the reaction to the DU implants (Figure 9 vs. Figure 3).

The capsules around the DU implants in the rats dying near the end of their normal life span were characterized histologically by fibrosis, inflammation, degeneration, and mineralization. Around the largest DU implants, the capsules were up to 0.5 mm thick and composed of dense fibrous tissue. More typically, the capsules were 0.1–0.2 mm thick. Black shards of corroded DU were embedded in the fibrous tissue capsules around the medium and large fragments. Smaller particles, in a range of sizes (<4 μm), were found in the capsule wall around all sizes of DU implants. Chronic inflammatory cells and particle-laden macrophages were frequently scattered throughout the capsule wall of the DU implants. Occasionally foreign-body giant cells were found. However, the amount of chronic inflammation in and around the capsules was generally similar with DU implants of all sizes. Degeneration of the fibrous tissue in the capsule wall was frequent at the interface with the implant. With this reaction, the tissue on the inner surface of the capsule was devitalized and necrotic. The lumen of the capsules contained necrotic and proteinaceous debris, scattered acute inflammatory cells, and varying amounts of black shards or particles. The particles were contained in macrophages or free in the lumen as amorphous clumps of various sizes. Mineralization of necrotic debris or devitalized fibrous tissue on the inner wall of the capsules was common.

The morphologic characteristics of the soft tissue tumors associated with the implants were further characterized (see Appendix C: Diagnostic Criteria for Soft Tissue Tumors and Appendix D: Characteristics of Implant-Associated Soft Tissue Tumors).

2. Morphologic – Radiographic Correlations

The tissue reactions around the DU implants can be correlated with the radiographic appearance of the DU implants. Radiographs on the day of implantation showed profiles of the DU implants with smooth edges and sharp corners (Figure 10A). The tissue reaction at 7 days after implantation, the earliest time point examined, showed that inflammation was present and that fibrosis had been initiated. Fine black particles were present in macrophages of the capsule (Figure 11A). In radiographs taken at 3 weeks after implantation, small, irregular radio-dense blebs extended from the edges of the implants, making them appear larger than at the time of implantation. The jagged appearance disrupted the sharp profile of the fragments and rounded the sharp corners (Figure 10B). The histologic reaction at 4 weeks showed a continued presence of inflammatory cells, but with at shift toward chronic inflammatory cells. Degeneration was at its peak at this time. The proteinaceous debris may have accounted for the jagged, irregular appearance of the implants in the radiographs at 3 weeks. Corrosion particles also continued to be present (Figure 11B). At 1 year after implantation, the radiographic profiles of the fragments were rounded, with no corners and a fine, jagged edge (Figure 10C). Histologically, fibrosis was prominent, but the number of inflammatory cells decreased. Acute inflammatory cells were few. Corrosion particles were present as well as large black corrosion fragments. Degeneration and mineralization of the capsule were also present at one year (Figure 11C).

3. Molecular Biomarkers of Neoplasia in DU- and Thorotrast®-Induced Soft Tissue Tumors

The results of the IHC determinations of p53, MDM2, p21, and c-myc, as well as the *BstN*1 assay for K-ras codon 12 mutations are shown in Appendix E for each tumor examined. The frequency of these molecular changes is summarized in Table 6. Expression of p53, indicative of p53 gene mutation, occurred in 3/11 (27%) of the DU-induced malignant soft tissue tumors tested and was significantly increased over the 0% incidence in the Thorotrast®-induced malignant soft tissue tumors (two-tailed, $p < 0.03$). The nuclear staining was fairly widespread in the positive tumors (Figure 12).

Table 6
Frequency[a] of Molecular Changes in Soft Tissue Tumors
Induced by DU or Thorotrast®

	p53 Expression	MDM2 Expression	c-myc Expression	p21 Expression	K-ras Mutation
DU	3/11[b]	1/11	0/8	1/9	0/6
Thorotrast®	0/25	2/25	2/20	2/23	0/20
Tantalum	1/2	1/2	1/1	1/2	0/1

[a]Number with positive expression/number examined.
[b]Significantly different from Thorotrast® (two-tailed, $p < 0.03$, Fisher's Exact test).

Only two tumors were induced by the tantalum implants, but one of these had positive nuclear staining for p53. The 50% frequency of p53 expression in the tantalum-induced tumors was greater than that of the Thorotrast®-induced tumors with borderline significance (two-tailed, $p < 0.08$).

The expression of MDM2, p21, and c-myc were 10% or less of the malignant tumors tested in all of the groups except for those implanted with tantalum which induce only two tumors. No mutation in K-ras codon 12 was noted in any of the tumors tested.

The frequency of molecular changes also appeared related to the tumor type, as classified by morphologic criteria (Table 7). Gene changes were more frequent in malignant fibrous histiocytoma than in osteosarcoma or fibrosarcoma. Of the six malignant fibrous histiocytomas induced by DU, three had p53 expression. However, none of these correlations was significant (two-tailed, $p > 0.05$).

Table 7
Frequency of Molecular Changes in Soft Tissue Tumors:
Relation to Tumor Type[a]

	p53	p21	MDM2	c-myc
Malignant fibrous histiocytoma	4/21	2/18	2/17	2/18
Fibrosarcoma	0/12	1/8	1/9	1/8
Osteosarcoma	0/3	1/3	1/3	0/3
Myoblastoma	0/1	0/1	0/1	ND

[a]No correlation with tumor type (two-tailed, $p > 0.50$, Fisher's Exact test).
ND = Not done

4. Molecular Biomarkers as Early Indicators of DU- and Thorotrast®-Induced Soft Tissue Tumors

The mutation of p53 was the only molecular biomarker for DU or Thorotrast®-induced neoplasia found among the five likely markers examined (Table 6). The frequency of p53 in the 11 DU malignant tumors was significantly increased over that of the Thorotrast® tumors but was found in only 27% of those tumors. The three tumors were all MFH. Two microscopic, but malignant, tumors in capsules and the one benign fibrous histiocytoma did not have cells with nuclear staining for p53 (Appendix E). Review of the histologic sections of capsules from all the rats in the serial sacrifice study did not reveal additional microscopic tumors or other proliferative lesions for evaluation.

5. Patterns of Gene Expression in DU- and Thorotrast®-Induced Soft Tissue Tumors

Data was collected by Phosphoimager scans and were analyzed with AtlasImage 2.7 and GeneSpring (Appendix F). Global normalization of each array was performed to account for hybridization efficiencies prior to comparison to the control array containing rat skeletal muscle. A control hybridization was performed for each of the four sets of hybridizations, which utilized a pooled normal rat skeletal muscle total RNA, thus allowing for variations in cDNA synthesis and hybridization efficiencies. Each group (a–d, Table 4) was hybridized to an individual array, and comparisons were made to the normal rat skeletal muscle. Gene expression values for each tumor type and induction by DU or Thorotrast® were calculated. An intensity cutoff ($I > 10$) was assigned as significantly present based upon visual inspection of the *tiff* images. Analysis was performed according to the flow chart in Figure 13.

Out of the initial 1,176 genes assayed 521 genes were significantly present in the RNA population queried. Comparison between each tumor type with normal rat skeletal muscle resulted in 76 genes which were significantly ($p < 0.05$) differentially present in at least one of the tumor types (Appendix F, Tables F.1–F.3). Fourteen genes were specific to Thorotrast®-induced fibrosarcoma (BA), 26 genes were specific to Thorotrast®-induced MFH (CA), and 19 genes were specific to DU-induced MFH (DA). A Venn diagram comparing the three tumor groups for significant genes ($p < 0.05$) is shown in Figure 14. The fibrosarcomas and MFH associated with Thorotrast® were the most alike, sharing in common 10 genes (middle and top intersection) that significantly differentiated between the tumors and skeletal muscle.

The next most similar category was the tumor type itself (MFH associated with either Thorotrast® or DU) sharing 7 genes (middle and right intersection) while the most dissimilar category included fibrosarcoma induced by Thorotrast® and MFH induced by DU, sharing only 4 genes (middle and left intersection).

The specific genes that were different among the various categories are shown in Tables F.1–F.3, Appendix F. Selected significantly expressed genes of interest are noted in Table 8a and include the expressed cell cycle genes, apoptosis genes, and genes related to proliferation. All the shared expressed genes are noted in Table 8b and in Table F.4 (Appendix F). Only two genes were shared by all categories, glyogenin and 40S ribosomal protein or FBR murine sarcoma virus ubiquitously expressed. The two types of tumors induced by Thorotrast® shared the most genes, eight.

Table 8a
Comparison of Genes Expressed in Tumors Induced by DU or Thorotrast® Implants
a. Exclusively Expressed Genes

Tumor Type	Number Exclusively Expressed	Total Number Expressed	Exclusively Expressed Genes (selected)
DU Tumors	19	28	G2/M-specific cyclin G T-complex protein 1 Growth factor-induced polypeptide, 53kDa Early growth response protein 3 Defender against cell death 1 protein (DAD1)
Thorotrast® Tumors	40	67	T-cell cyclophilin junD proto-oncogene Carcinoembryonic antigen-related protein CGM1 Growth-related c-myc-responsive protein RCL Laminin alpha3 subunit (LAMA3) Vimentin TAP-related matrix metalloproteinase 10 Tissue inhibitor of metalloproteinase 1 (TIMP1)

Significant expression compared to muscle tissue ($p < 0.05$).

Table 8b
Comparison of Genes Expressed in Tumors Induced by DU or Thorotrast® Implants
b. Shared Expressed Genes

Tumor Types	Number Shared	Total Number Expressed	Shared Genes
DU MFH and Thorotrast® MFH Tumors	7	69	Glycogenin 40S ribosomal protein S30 (RPS30); Finkel-Biskis-Reilly murine sarcoma virus ubiquitously expressed (FAU; FUB1) Laminin receptor 1 40S ribosomal protein S3 (RPS3) Fibroblast growth factor receptor 4 (FGFR4) Thiol-specific antioxidant protein (1-Cys peroxiredoxin) cAMP-dependent protein kinase catalytic subunit
All DU Tumors and all Thorotrast® Tumors	9	95	(the above 7 plus-) Presenilin 2 (PSEN2; PSNL2; PS2); apoptosis-linked gene 3 (ALG3); Alzheimer disease 4 homolog (AD4H) Skeletal muscle alpha-actin; alpha-actin 1 (ACTA1)

Significant expression compared to muscle tissue ($p < 0.05$).

Determination significant gene expression using a p value <0.05 necessitates a signal intensity of greater than 10 in all comparisons, thus genes whose expression is absent in one category are excluded from analysis. Therefore, a separate query was performed to capture genes whose expression were present in a tumor category but absent in normal rat skeletal muscle and those whose expression were present in normal rat skeletal muscle but absent in a tumor category. A second Venn diagram (Figure 15) demonstrates the comparison of expressed genes not found in control muscle. Twenty-nine genes were present in the tumors whose expression was absent in normal rat skeletal muscle. A third Venn diagram (Figure 16) illustrates the comparison genes absent in tumors but present in normal rat skeletal muscle. Nineteen genes were found in this category.

C. Discussion

1. Morphologic Characteristics of the Capsules and Tumors

Tissue reaction around the DU implants was obvious at 7 days and continued through 18 months after implantation. Acute and chronic inflammation was prominent at 7 days after implantation. The inflammation was still prominent at 1 month but waned at 2 months and remained so until 18 months after implantation. Fibrosis, initially seen at 7 days, increased over

this time. Degeneration of the capsule wall was present at 7 days and persisted, becoming mineralized at later times. Small particles of corroded DU were found in the capsules as early as 7 days after implantation. In addition, shards of DU were found in the wall of the capsules at 6 months on through 18 months.

These tissue reactions to DU implants in rats generally follow the time course of inflammation, wound healing, and foreign-body response as classically outlined (Anderson *et al.*, 1996). With DU the chronic inflammation with fibrosis follows the acute inflammation relatively rapidly and continues for life span. Although persistent, the inflammation is not particular severe. The feature of degeneration with subsequent mineralization is not one included with the classical description of foreign-body responses. An important phenomenon following implantation of DU in the tissues is the marked corrosion and fragmentation of the DU that occurs within days and continues for the life span of the rats. The corrosion may well cause a redox reaction at the interface of the implant leading to degeneration of the adjacent tissue (Steinemann, 1996). This phenomenon may also play a role in the persistence of the low-grade inflammation and the production of a fibrous capsule.

The tissue reactions to silicone implants in rats are similar to those to DU implants. The early (2 months) reaction to silicone implants has been compared with a positive control (impermeable cellulose filters) and a negative control (porous cellulose filters) (James *et al.*, 1997). The inflammatory response to the carcinogenic cellulose and silicone implants was attenuated and associated with the formation of a thick fibrotic capsule (measuring 0.21–0.27 mm thick). In contrast, the porous cellulose filters induced a markedly different cellular response in which the inflammatory reaction was more extensive, prolonged, and associated with minimal fibrosis (capsules 0.08 mm thick). The reactions to the DU implants were closer to that of the carcinogenic silicone and impermeable cellulose filters. The capsules around the DU implants averaged 0.1–0.2 mm thick. The inflammation, although persistent, was not marked in intensity. In addition, the multinucleate giant cell accumulation described as being marked around the negative control implants were rarely seen around the DU implants.

The tissue reactions and their effect on the DU implants could be seen on radiographs. There was a correlation of the jagged, irregular radiographic appearance of the implants at 3 weeks and the present of inflammation and degeneration in the tissue sections. At 1 year the rounded outline of the implants correlated with the large fragments and shards of DU

created by corrosion of the implants. If radiographs can be used to visualize these reactions to DU in humans as they can in rats, they may provide an important technique to determine the progression of the lesions and aid in treatment plans for individuals with embedded DU fragments.

2. Molecular Markers of Neoplasia

Molecular changes were detected at a low frequency for all malignant tumors tested except for K-ras mutations. The expression of MDM2, c-myc, and p21 were not significantly different between the groups implanted with DU and those injected with Thorotrast®.

The nuclear staining for p53, indicative of a mutation in this oncogene, was increased in 27% malignant tumors associated with DU implants. The increase was significantly increased over the Thorotrast®-induced tumors, none of which had nuclear staining for p53. The two tumors in capsules and the one benign fibrous histiocytoma did not stain for p53. This lack of p53 staining in small or benign tumors does not support the ideas that p53 is an important early molecular change in the pathway to soft tissue sarcomas induced by DU. However, the numbers of small tumors available for testing is too small to yield statistically significant results based on the 27% incidence of p53 gene changes in the soft tissue sarcomas.

The lack of K-ras codon 12 mutations was not expected. K-ras mutations are the most frequent mutations in rodent tumors (Sills *et al.*, 1999), and mutations of codon 12 are the most frequent of the K-ras mutations. Because of this, sequencing of codons 12 and 13 of some tumors was initiated to verify the *BstN*1 results. The sequences were approximately 80 base-pairs long and included codons 12 and 13, but did not extend to codon 61. No mutations were present in codon 12 or 13. This result verified the RFLP analysis using the *BstN*1 test.

3. Patterns of Gene Expression in Tumors

The patterns of gene expression in the tumors induced by DU and by Thorotrast showed little similarity. Nineteen genes were exclusively expressed (significantly increased over control) in the DU-induced tumors and 40 were exclusively expressed in the Thorotrast-induced tumors. Several of these genes are related to cell proliferation and neoplasia (i.e., DAD, growth factor-induced polypeptide, junD proto-oncogene and cyclin G, see Table 8a). Several of the exclusively expressed genes related to tumor cell type (i.e., laminin and

vimentin) and others to tumor growth (i.e., matrix metalloproteinase and tissue inhibitor of metalloproteinase, see Table 8b). Only nine genes were shared by the tumors induced by the two types of implants. Only three of these, FBR murine sarcoma virus ubiquitously expressed, fibroblast growth factor receptor 4, and apoptosis-linked gene 3 appeared related to proliferative or neoplastic processes.

Although some proliferative or neoplasia-related genes were shared or exclusively expressed, no bone fide pattern of causation could be detected (Hanahan and Weinberg, 2000). Several factors may account for this observation. The technique of microarrays may not be sensitive enough to detect small changes in gene expression. Many more genes were exclusively expressed rather than shared. This may relate to the different tissue environments of the DU- and Thorotrast-induced tumors. The DU was surrounded by a thick connective tissue capsule with inflammation and degeneration. In contrast, the Thorotrast invoked little reaction in the tissues. The lack of similarity of gene patterns may be evidence that the mechanism of neoplasia initiated by DU and Thorotrast may be different.

4. Hypothesis Testing

1. Patterns of gene expression in soft tissue sarcomas associated with implanted DU differ from the patterns in sarcomas induced by injected Thorotrast®.

This hypothesis is true based on the finding of p53 expression only in the DU and tantalum-induced tumors and the lack of similarity of differential gene expression.

2. The specific oncogenes and tumor suppressor genes in soft tissue sarcomas associated with implanted DU will be expressed in the capsules that surround DU and are antecedent lesions to the sarcomas.

This hypothesis cannot be proven true. The 27% incidence of p53 mutations in the grossly visible tumors is not sufficiently high to accurately predict the incidence in the small number of microscopic tumors in the capsules and in the benign tumors available.

3. Novel tumor genes expressed in the soft tissue sarcomas associated with implanted DU and injected Thorotrast® will be expressed in the capsules that surround DU and are precursor lesions to the sarcomas.

This hypothesis could not be fully tested as the Statement of Work was modified subsequent to the peer review of the project on Dec. 5–6, 2002, organized by the American Institute of Biological Sciences. However, no novel genes were found in the tumor samples by using a microarray for differential gene expression.

III. KEY RESEARCH ACCOMPLISHMENTS

- Demonstrated that corrosion of DU implants occurs within 7 days after implantation and correlates with tissue reactions that are detectable with radiographs.
- Determined that DU-induced soft tissue sarcomas in rats have a 27% frequency of p53 gene expression.
- Determined that DU-induced soft tissue tumors in rats have a significantly higher frequency of p53 molecular changes than Thorotrast®-induced tumors. This suggests a different mechanism of carcinogenic action.
- Determined that DU-induced soft tissue tumors in rats have a low frequency of MDM2, c-myc, and p21 gene expression and no K-ras codon 12 mutations.
- Determined that patterns of gene expression are not similar between tumors induced by DU and Thorotrast®, further evidence of a different mechanism of carcinogenic action for these two carcinogens.

IV. REPORTABLE OUTCOMES

Publication:

Hahn, F. F., R. A. Guilmette and M. D. Hoover (2002). Implanted depleted uranium fragments cause soft tissue sarcomas in the muscles of rats. *Environ. Health Perspect.110*: 51–59.

Presentations:

Hahn, F. F. and R. A. Guilmette. Carcinogenicity of Depleted Uranium Fragments in Wistar Rats. Presented at the Society of Toxicology Annual Meeting, March 2002, Nashville, TN.

Hahn, F. F. and R. A. Guilmette. Depleted Uranium Metal Implants are Carcinogenic in Rats. Presented at a workshop: Questions Surrounding Depleted Uranium Toxicity: Answers from the Clinic and the Laboratory, Society of Toxicology Annual Meeting, March 2003, Salt Lake City, UT.

V. CONCLUSIONS

These studies in rats show that DU (0.75% Ti) rapidly corrodes when embedded in muscle. In 7 days corrosion, and the acute tissue reaction to it, can be visualized in radiographs of the tissues. Corrosion continues for the 2-year life span of the rats causing an enlargement of the embedded DU on radiographs, although the chronic tissue reaction cannot be visualized. This information may be useful in interpreting radiographs of DU materials embedded in humans.

The mechanisms of cancer may be different in tumors induced by DU and those induced by Thorotrast®, an agent known to induce cancer by radiation mechanisms. DU soft tissue tumors have a significantly increased expression of p53 (which is related to mutation of the p53 oncogene) when compared to Thorotrast® soft tissue tumors which have not expression of p53. In addition, the patterns of gene expression in tumors induced by the two agents are dissimilar. This information on mechanism of cancer induction may be important in determining what populations of exposed humans might be used for assessment of risk for soldiers wounded with DU fragments.

These studies were not able to determine a molecular change that might be an early indicator of cancer around an embedded fragment of DU. A mutation in the oncogene p53 is that potential but insufficient numbers of small tumors were present in the materials from the original life-span study in rats. Further studies with tumor materials generated specifically for the purpose of detected early changes would be needed.

VI. PERSONNEL

Fletcher F. Hahn, DVM, PhD. Principal Investigator, Pathology Group Head, Experimental Toxicology Program, Senior Scientist

Steven A. Belinsky, PhD. Program Manager, Molecular Biology and Lung Cancer Program; Senior Scientist

Susan E. Boggs, PhD. Molecular Biologist, Respiratory Immunology and Asthma Program, Associate Research Scientist

VII. REFERENCES

Anderson, J. M., A. G. Gristina, S. R. Hanson, L. A. Harker, R. J. Johnson, K. Merritt, P. T. Naylor and F. J. Schoen (1996). Chapter 4, Host reactions to biomaterials and their evaluation. In *Biomaterials Science, An Introduction to Materials in Medicine* (B. D. Ratner, A. S. Hoffman, F. J. Schoen and E. Lemons, eds.), pp. 165-214, Academic Press, San Diego.

Barrios, C., J. S. Castresana, J. Ruiz and A. Kreicberbs (1994). Amplification of the c-myc proto-oncogene in soft tissue sarcomas. *Oncology 51:* 13–17.

Belinsky, S. A., S. K. Middleton, S. M. Picksley, F. F. Hahn and K. J. Nikula (1996). Analysis of the K-ras and p53 pathways in X-ray-induced lung tumors in the rat. *Radiat. Res. 145*: 449-456.

Belinsky, S. A., D. S. Swafford, G. L. Finch, C. E. Mitchell, G. Kelly, F. F. Hahn, M. W. Anderson and K. J. Nikula (1997). Alterations in the K-*ras* and *p53* genes in rat lung tumor. *Environ. Health Perspect. 105(Suppl. 4)*: 901–906.

Belinsky, S. A., K. J. Nikula, W. A. Palmisano, R. Michels, G. Saccomano, E. Gabrielson, S. B. Baylin and J. G. Herman (1998). Aberrant methylation of a p16 (INK4a) is an early event in lung cancer and a potential biomarker for early diagnosis. *Proc. Natl. Acad. Sci. USA 95*: 11891–11896.

Buchholz, T. A., K. McCabe, J. Cobb, H. Haroff, B. R. Prestidge and W. J. Ehler (1999). TP53 overexpression in radiation-induced osteosarcomas of the rabbit mandible. *Radiat. Res. 151*: 278–282.

Castresana, J. S., C. Barrios, L. Gomez and A. Kreicbergs (1994). No association between c-myc amplification and TP53 mutation in sarcoma tumorigenesis. *Cancer Genet. Cytogenet. 76*: 47–49.

Cordon-Cardo, C., E. Latres, M. Drobnjak, M. R. Oliva, D. Pollack, J. M. Woodruff, V. Marechal, J. Chen, M. F. Brennan and A. J. Levine (1994). Molecular abnormalities of MDM2 and p53 genes in adult soft tissue sarcomas. *Cancer Res. 54*: 794–799.

Dong, S. M., G. Johnson, L. Geng, R. Favis, K. Boyton, K. Hibi, S. N. Goodman, M. D'Allessio, P. Paty, S. R. Hamilton, D. Sidransky, F. Barany, B. Levin, A. Shuber, K. W. Kinzler, B. Vogelstein and J. Jen (2001). Detecting colorectal cancer in stool with the use of multiple genetic targets. *J Natl. Cancer Inst. 93*: 858–865.

Enzinger, F. M. and S. W.Weiss (1995). Benign tumors of the peripheral nerves. In *Soft Tissue Tumors, Third Edition* (F. M. Enzinger and S. W.Weiss, eds.), pp. 821–888, Mosby Year Book, Inc., St. Louis, MO.

Greaves, P. (1997). Soft tissue tumors including cardiovascular lesions. In *Pathology of Neoplasia and Preneoplasia in Rodents, EULEP Color Atlas, Vol. 2* (P. Bannasch and W. Gössner, eds.), pp. 183–202, Schattauer, Stuttgart.

Hahn, F. F., R. A. Guilmette and M. D. Hoover (2000). Toxicity of depleted uranium fragments in Wistar rats. *Health Phys. 78*: S129.

Hahn, F. F., R. A. Guilmette and M. D. Hoover (2002). Implanted depleted uranium fragments cause soft tissue sarcomas in the muscles of rats. *Environ. Health Perspect. 110*: 51-59, 2002.

Hanahan, D. and R. A. Weinberg (2000). The hallmarks of cancer. *Cell 100*: 57-70.

Huff, J. (1999). Value, validity, and historical development of carcinogenesis studies for predicting and confirming carcinogenic risks to humans. In *Carcinogenicity: Testing, Predicting and Interpreting Chemical Effects* (K. T. Kitchin, ed.), pp. 21–123, Marcel Dekker, Inc., New York.

James, S. J., M. Pogribna, B. J. Miller, B. Bolon and L. Muskhelishvili (1997). Characterization of cellular response to silicone implants in rats: Implications for foreign-body carcinogenesis. *Biomaterials 18(9)*: 667-675.

Kamikawa, T., M. Amenomori, T. Itoh, H. Momoi, H. Hiai, R. Machinami, T. Ishikawa, T. Mori, Y. Shimahara, T. Yamaoka and M. Fukumoto (1999). Analysis of genetic changes in intrahepatic cholangiocarcinoma induced by thorotrast. *Radiat. Res. 152*: S118–S124.

Khan, J., R. Simon, M. Bittner, Y. Chen, S. B. Leighton, T. Pohida, P. D. Smith, Y. Jiang, G. C. Gooden, J. M. Trent and P. S. Meltzer (1998). Gene expression profiling of alveolar rhabdomyosarcomas with cDNA microarrays. *Cancer Res. 58*: 5009–5013.

Kuwashima, Y., N. Nemoto and T. Ishikawa (1993). Expression of protooncogenes and cytoskeletal actin gene in foreign body-induced murine sarcomas. *In Vivo 7*: 139–142.

Leach, F. S., T. Tokino, P. Meltzeer, M. Burrell, J. D. Oliner, S. Smith, D. E. Hill, D. Sifransky, K. W. Kinzler and B. A. Vogelstein (1993). p53 Mutation and MDM2 amplification in human soft tissue sarcomas. *Cancer Res. 53*: 2231–2234.

Levi, A., R. Urbano-Ispizua, R. Gill, D. M. Thomas, T. J. Gilbertson, C. Foster and C. J. Marshall (1991). Multiple K-*ras* codon 12 mutations in cholangiocarcinomas demonstrated with a sensitive polymerase chain reaction technique. *Cancer Res. 51*: 3497–3502.

MacDonald, J. S. and H. H. Scribner (1999). The maximum tolerated dose and secondary mechanisms of carcinogenesis. In *Carcinogenicity: Testing, Predicting and Interpreting Chemical Effects* (K. T. Kitchin, ed.), pp. 125–144, Marcel Dekker, Inc., New York.

'McDiarmid, M. A., J. P. Keogh, F. J. Hooper, K. McPhaul, K. Squibb, R. Kane, R. DiPino, M. Kabat, B. Kaup, L. Anderson, D. Hoover, L. Brown, M. Hamilton, D. Jacobson-Kram, B. Burrows, and M. Walsh (2000). Health effects of depleted uranium on exposed Gulf War veterans. *Environ. Res. Sec. A 82*: 168–180.

McDiarmid, M. A., S. Engelhardt, M. Oliver, P. Gucer, P. D. Wilson, R. Kane, M. Kabat, B. Kaup, L. Anderson, D. Hoover, L. Brown, B. Handwerger, R. J. Albertini, D. Jacobson-Kram, C. D. Thorne and K. S. Squibb (2004). Health effects of depleted uranium on exposed Gulf War veterans: A 10-year follow-up. *J. Toxicol. Environ. Health A 67*: 277–296.

McDonnell, T. L., R. Montes de Oca Luna, S. Cho, L. L. Amelse, A. Chaves-Reyes and G. Lozano (1999). Loss of one but not two mdm2 null alleles alters the tumour spectrum in p53 null mice. *J. Pathol. 188*: 322–328.

Miller, A. (1988). Depleted uranium health effects: Transformation, mutagenicity and carcinogenicity. In *Health Effects of Embedded Depleted Uranium Fragments* (D. R. Livengood, ed.), AFRRI Special Publication 98-3, pp. 11–13.

Miller, A. C., W. F. Blakely, D. Livengood, T. Whittaker, J. Xu, J. W. Ejnik, M. M. Hamilton, E. Parlette, T. St. John, H. M. Gerstenberg and H. Hsu (1998b). Transformation of human osteoblast cells to the tumorigenic phenotype by depleted uranium-uranyl chloride. *Environ. Health Perspect. 106*: 465–471.

Molina, R., A. Pellin, S. Navarro, J. Boix, C. Cards and A. Llombart-Bosch (1999). Analysis of p53 and MDM2 proteins in malignant fibrous histiocytoma in absence of gene alteration. *Virchows Arch. 435*: 596–605.

Momand, J., G. P. Zambetti, D. C. Olson, D. George and A. J. Levine (1992). The mdm2 oncogene product forms a complex with the p53 protein and inhibits p53 transactivation. *Cell 69*: 1237–1245.

Mousses, S., L. McAuley, R. S. Bell, R. Kandel and I. L. Andrulis (1996). Molecular and immunohistochemical identification of p53 alterations in bone and soft tissue. *Mod. Pathol. 9*: 1–6.

Nickell-Brady, C., F. F. Hahn, G. L. Finch and S. A. Belinsky (1994). Analysis of K-ras, p53, and c-raf-1 mutations in beryllium-induced rat lung tumors. *Carcinogenesis 15(2)*: 257–262.

Niwa, O., Y. Enoki and K. Yokoro (1998). Overexpression and amplification of the c-myc gene in mouse tumors induced by chemicals and radiations. *Jpn. J. Cancer Res. 80*: 212–218.

Reid, A. H., M. M. Tsai, D. J. Venzon, C. F. Wright, E. E. Lack and T. J. O'Leary (1996). MDM2 amplification, P53 mutation, and accumulation of the P53 gene product in malignant fibrous histiocytoma. *Diagn. Mol. Pathol. 5*: 65–73.

Selvanayagam, C. S., C. M. Davis, M. N. Cornforth and R. L. Ullrich (1995). Latent expression of p53 mutations and radiation-induced mammary cancer. *Cancer Res. 55*: 3310–3317.

Sills, R. C., G. A. Boorman, J. E. Neal, H. L. Hong and T. R. Devereux (1999). Mutations in ras genes in experimental tumors in rodents. In *The Use of Short- and Medium-Term Tests for Carcinogenesis and Data on Genetic Effects in Carcinogenic Hazard Evaluation* (D. B. McGregor, J. M. Rice and S. Venitl, eds.), IARC Scientific Publications No. 146, pp. 55–86, International Agency for Research on Cancer, Lyon.

Soini, Y., K. Vahakangas, K. Nuorva, D. Kamel, D. P. Lane and P. Paakko (1992). p53 Immunohistochemistry in malignant fibrous histiocytomas and other mesenchymal tumours. *J. Pathol. 168*: 29–33.

Stefanou, D. G., A. V. Nonni, G. Kalpouzos, A. Evangelou and N. J. Agnantis (1998). Immunophenotype, ras oncogenes and p53 onco-suppressor gene in benzo(a)pyrene induced malignant soft tissue tumours in Wistar rats. *In Vivo 12*: 511–521.

Steinemann, S. G. (1996). Metal implants and surface reactions. *Injury 27(Suppl. 3)*: S-C16-22.

Swafford, D. S., K. J. Nikula, C. E. Mitchell and S. A. Belinsky (1995). Low frequency of alterations in p53, K-ras, and mdm2 in rat lung neoplasms induced by diesel exhaust or carbon black. *Carcinogenesis 16*: 1215–1221.

Szadowska, A., B. Olborski, B. Harezga-Bal and M. Debiec-Rychter (1999). Expression of P53, MDM2 and Ki-67 antigens in soft tissue sarcomas. *Pol. J. Pathol. 50*: 9–16.

Taubert, H., P. Wurl, A. Meye, D. Berger, B. Thamm, K. Neuman, R. Hinze, H. Schmidt and F. W. Rath (1995). Molecular and immunohistochemical p53 status in liposarcoma and malignant fibrous histiocytoma: Identification of seven new mutations for soft tissue sarcomas. *Cancer 76*: 1187–1196.

Taubert, H., A. Meye, M. Bache, R. Hinze, H. J. Hozhausen, H. Schimidt, F. W. Rath, J. Dunst and P. Wurl (1998). p53 Status in radiation-induced soft-tissue sarcomas. *Strahlenther. Onkol. 174*: 427–430.

Wadayama, B., J. Toguchida, T. Tamaguchi, M. S. Sasaki and T. Yamamuro (1993). p53 Expression and its relationship to DNA alterations in bone and soft tissue sarcomas. *Br. J. Cancer 68*: 1134–1139.

Wilke, W., M. Maillet and R. Robinson (1993). H-ras-1 point mutations in soft tissue sarcomas. *Mod. Pathol. 6*: 129–132.

Yoo, J., H. K. Lee, C. S. Kang, W. S. Park, J. Y. Lee and S. I. Shim (1997). p53 Gene mutations and p53 protein expression in human soft tissue sarcomas. *Arch. Pathol. Lab. Med. 121*: 395–399.

VIII. APPENDICES

APPENDIX A

Acronym and Symbol Definition

*BstN*1 – Molecular test for K-ras

cDNA – Complementary DNA

c-myc – An oncogene

COD – Cause of death

DNA – Deoxyribonucleic acid

DU – Depleted uranium alloyed with 0.75% titanium

IHC – Immunohistochemistry

Inc – Incidental

K-ras – An oncogene

ln – Lymph node

LRRI – Lovelace Respiratory Research Institute

MDM2 – A protein that degrades p53

MFH – Malignant fibrous histiocytoma

NBF – Neutral buffered formalin

p21 – A cellular protein that inhibits normal cell cycling

p53 – A protein with tumor suppressor properties, mutation inactivates the suppression

PAS – Periodic Acid Schiff

PCR – Polymerase chain reaction

PTAH – Phosphotungstic acid hematoxylin, histochemical stain for muscle fibers

RFLP – Restriction fragment length polymorphism

RNA – Ribonucleic acid

Ta – Tantalum

Ti – Titanium

APPENDIX B

Figures

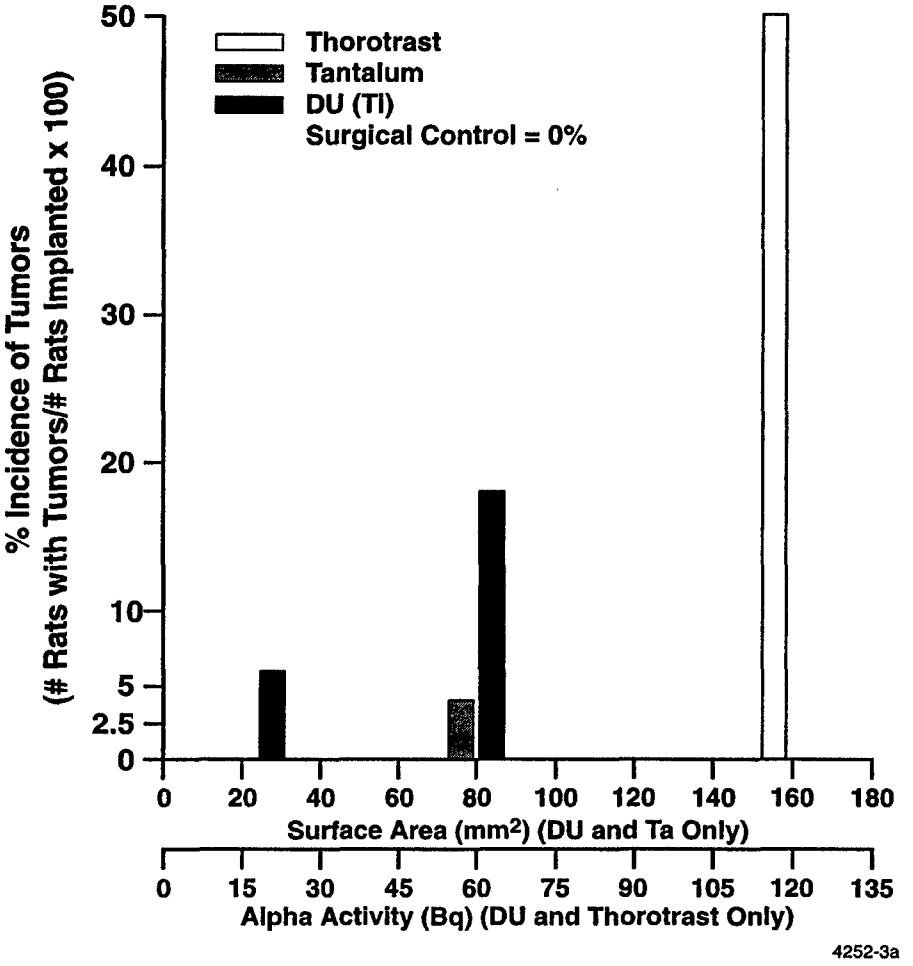

Figure 1. Incidence of soft tissue tumors in rats implanted with DU, Ta, or Thorotrast®. The incidence of tumors in rats with 5.0 x 5.0 mm DU fragments was significantly increased over the incidence in rats with Ta fragments of the same size. The positive control, Thorotrast®, produced the highest incidence of tumors.

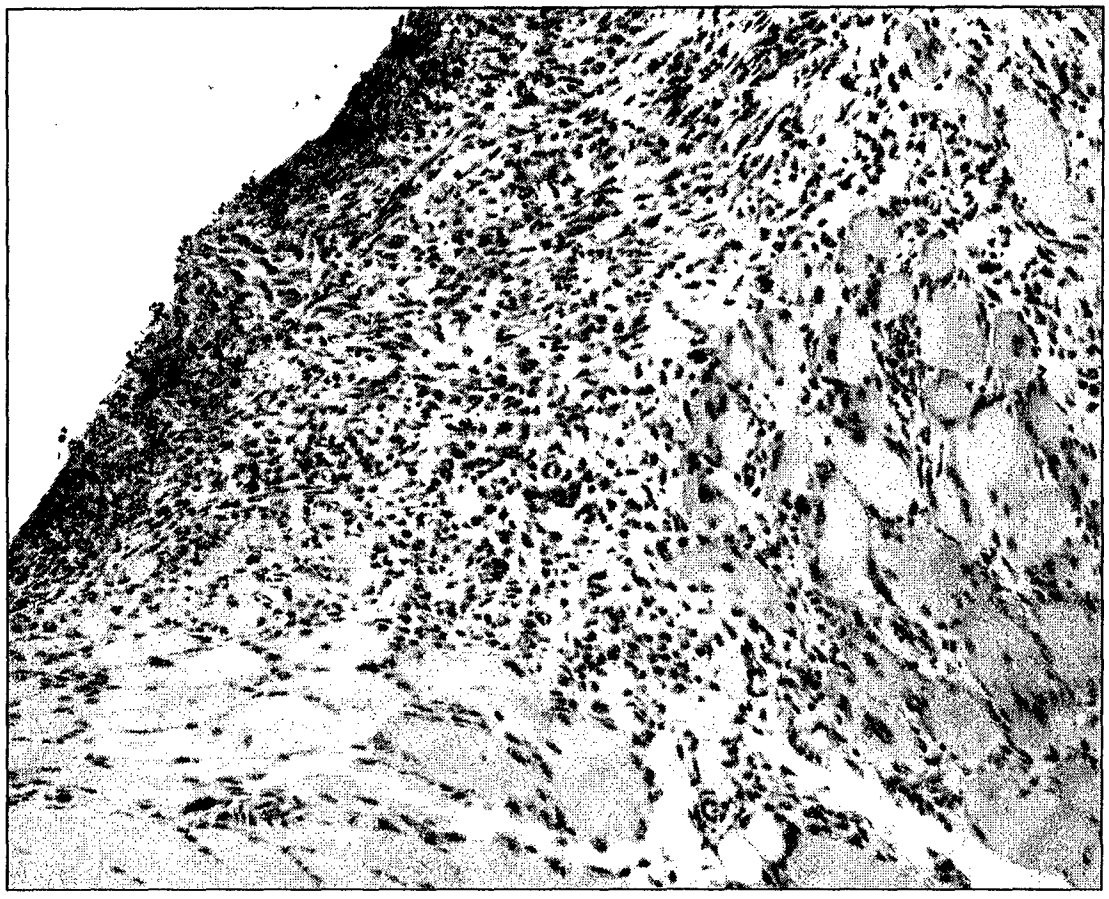

Figure 2. Acute inflammatory reaction with early fibroplasia around a 2.5 x 2.5 mm DU implant 7 days after implantation (Rat T031, H&E staining, 10X).

Figure 3. Chronic inflammation with necrotic debris and corrosion fragments around a 2.5 × 2.5 mm DU implant 18 months after implantation (Rat T055, H&E staining, 10X).

Figure 4. Small black corrosion particles in macrophages at 7 days after implantation (Rat T039, H&E staining, 20X).

Figure 5. Large black corrosion fragments of DU in the fibrous capsule 6 months after implantation (Rat T025, H&E staining, 10X).

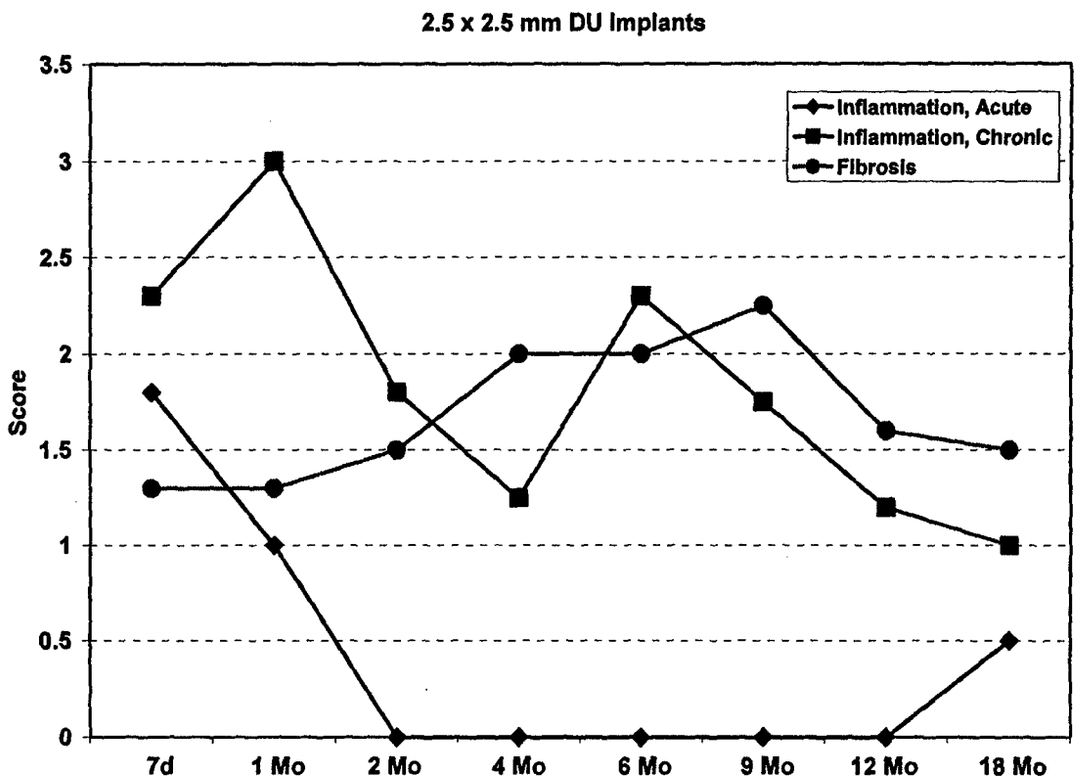

Figure 6. Inflammation and fibrosis around 2.5 x 2.5 mm DU fragments from 7 days to 18 months after implantation. Starting at 7 days inflammation and early fibrosis was prominent around the implants. Acute inflammation waned by one month.

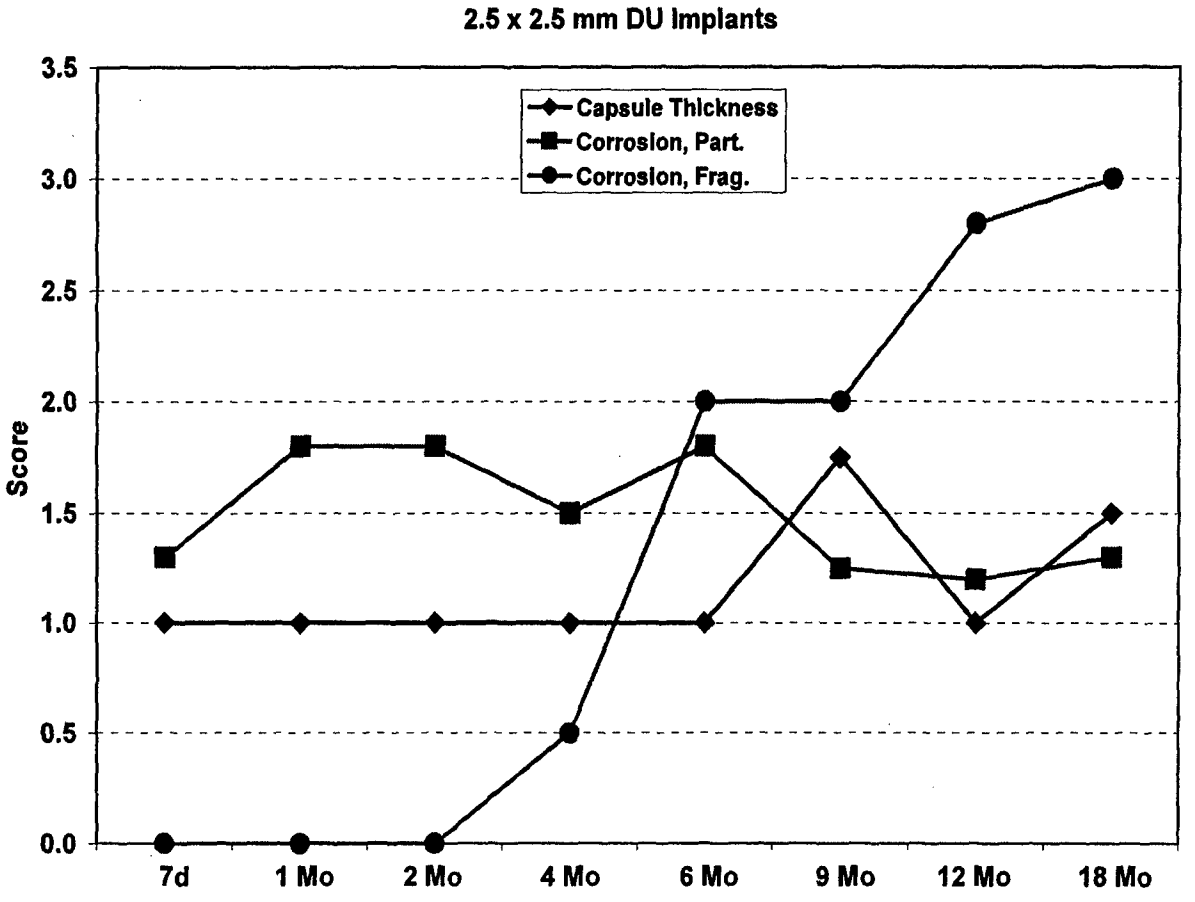

Figure 7. Corrosion of 2.5 × 2.5 mm DU fragments from 7 days to 18 months after implantation. Small, microscopic black particles were visible in the wall of the capsule at 7 days and continuing through 18 months. Large black fragments or shards, visible with the naked eye, were seen at 4 months after implantation and increased in amount through 18 months.

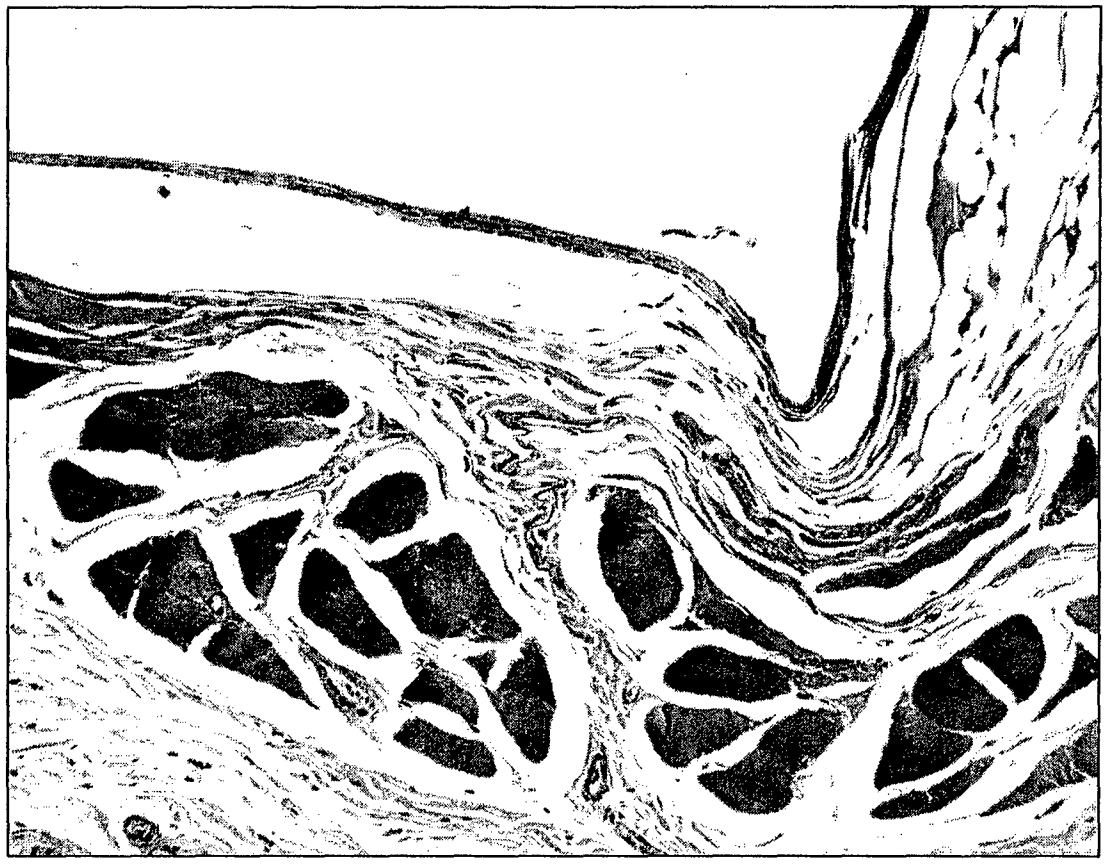

Figure 8. A very thin connective tissue capsule around a 5 × 5 mm Ta implant at 13 months after implantation (Rat B030, H&E staining, 10X).

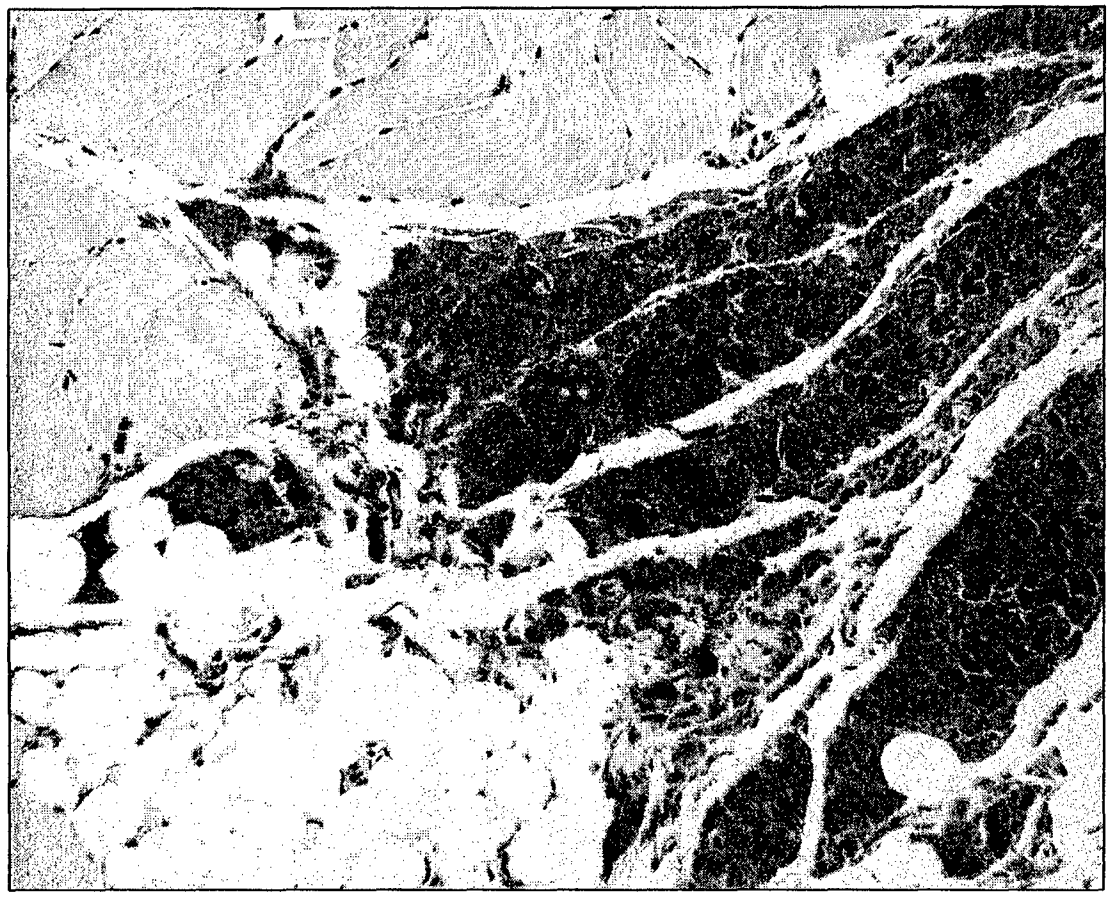

Figure 9. Accumulation of Thorotrast®-filled macrophages and little additional tissue reaction at injection site 12 months after injection (Rat O043, H&E staining, 10X).

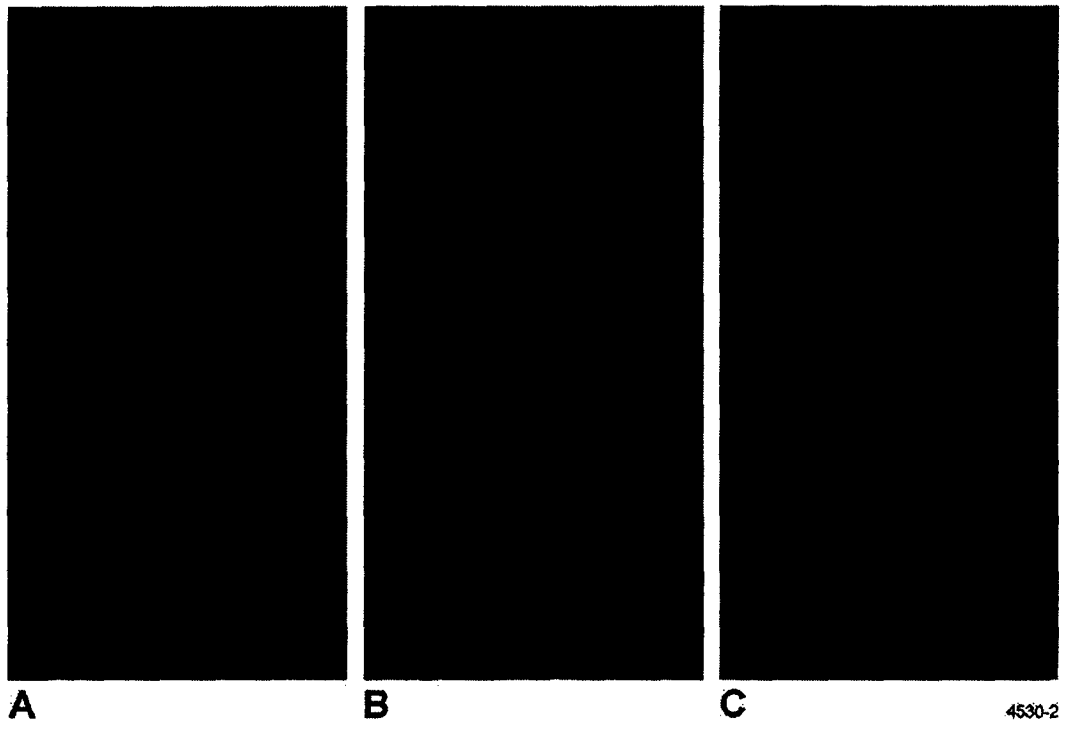

Figure 10. Radiograph of 5.0 × 5.0 × 1.5 mm DU implants: (A) on day of implantation, (B) 3 weeks after implantation, and (C) 1 year after implantation.

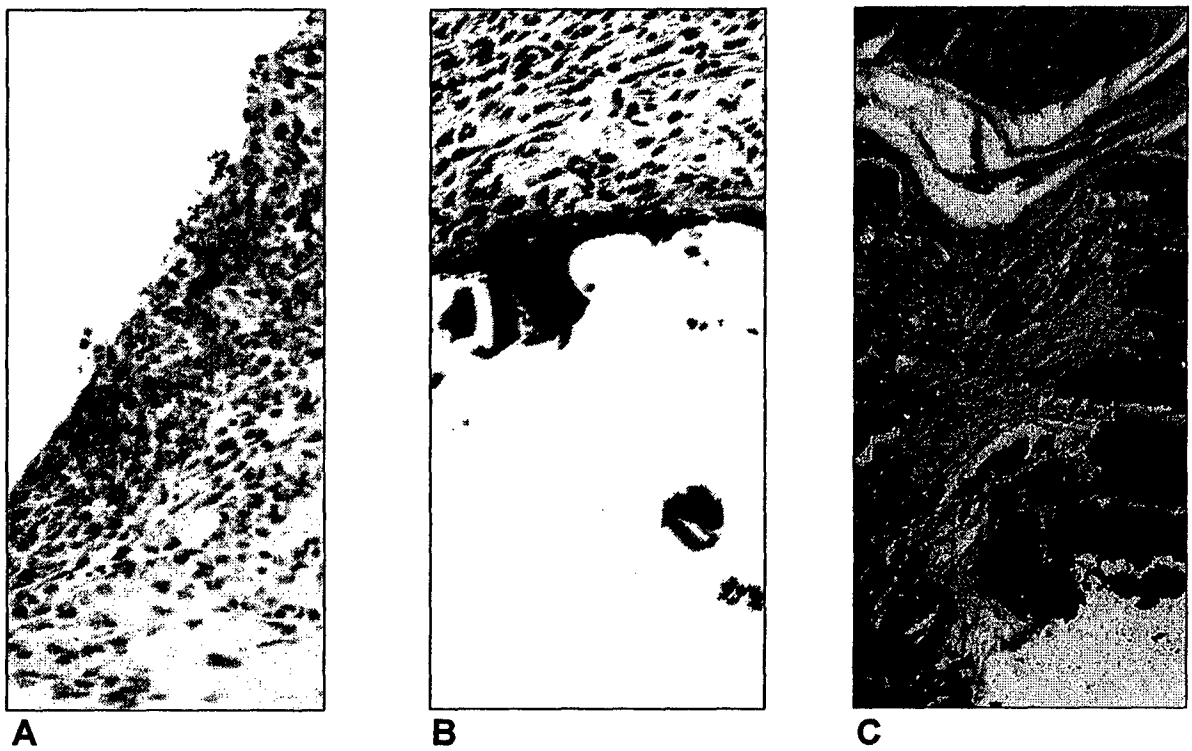

Figure 11. Tissue reaction to DU implants (A) 1 week after implantation, (B) 4 weeks after implantation, and (C) 12 months after implantation.

Figure 12. Positive immunohistochemical reaction in the cell nuclei showing the presence of a mutated p53 protein in a DU-induced soft tissue sarcoma (Rat E071, p53 immunohistochemistry with hematoxylin counterstain, 20X).

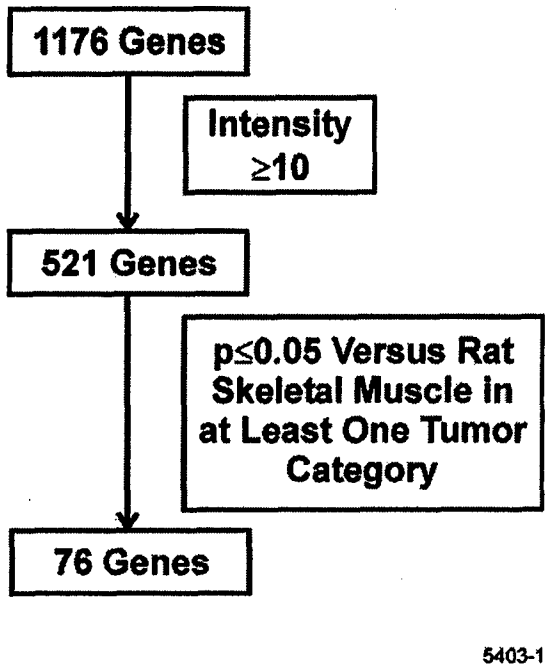

Figure 13. Flow of analyses of differentially-expressed genes.

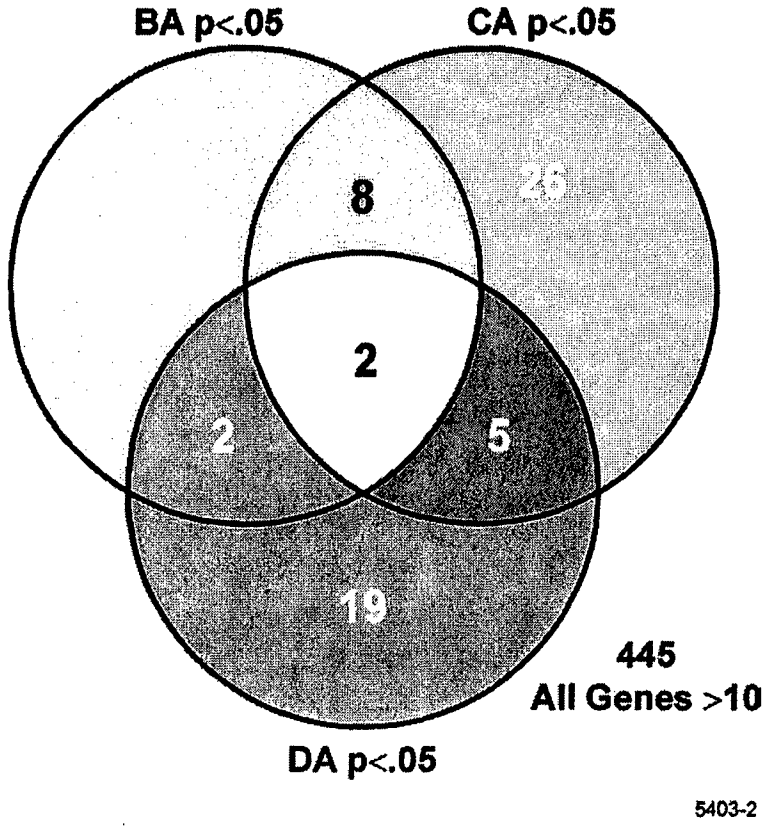

Figure 14. Venn diagram of differentially-expressed genes compared to normal rat skeletal muscle ($p < 0.05$). (A = skeletal muscle, B = Thorotrast® fibrosarcomas, C = Thorotrast® MFH, D = DU MFH)

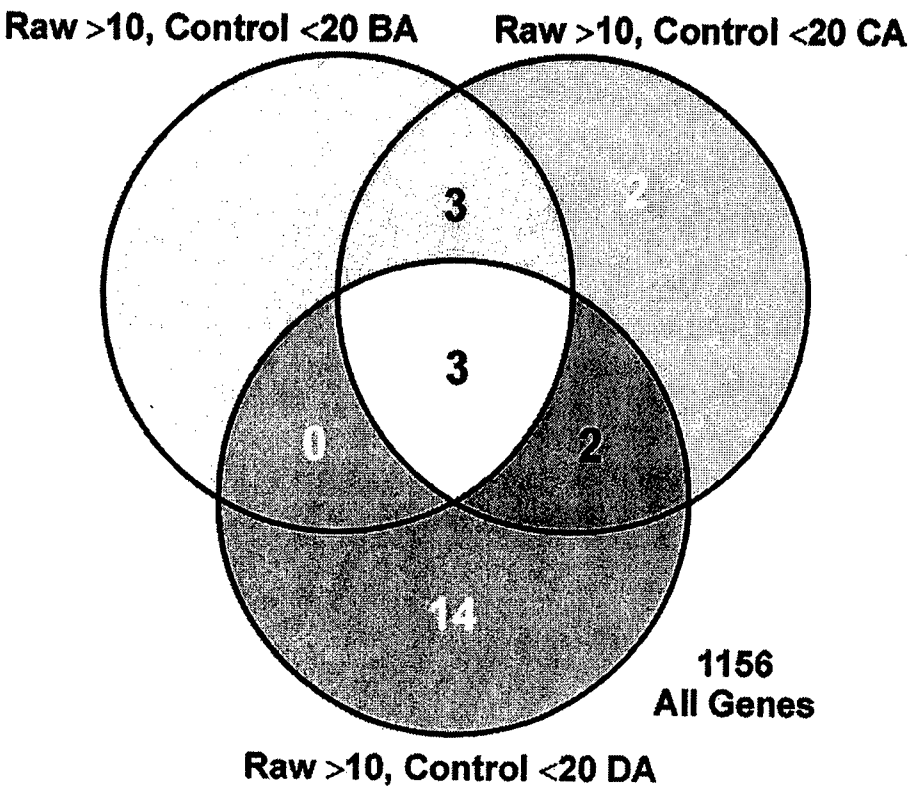

Figure 15. Venn diagram of genes expressed in tumors, but absent in muscle. (A = skeletal muscle, B = Thorotrast® fibrosarcomas, C = Thorotrast® MFH, D = DU MFH)

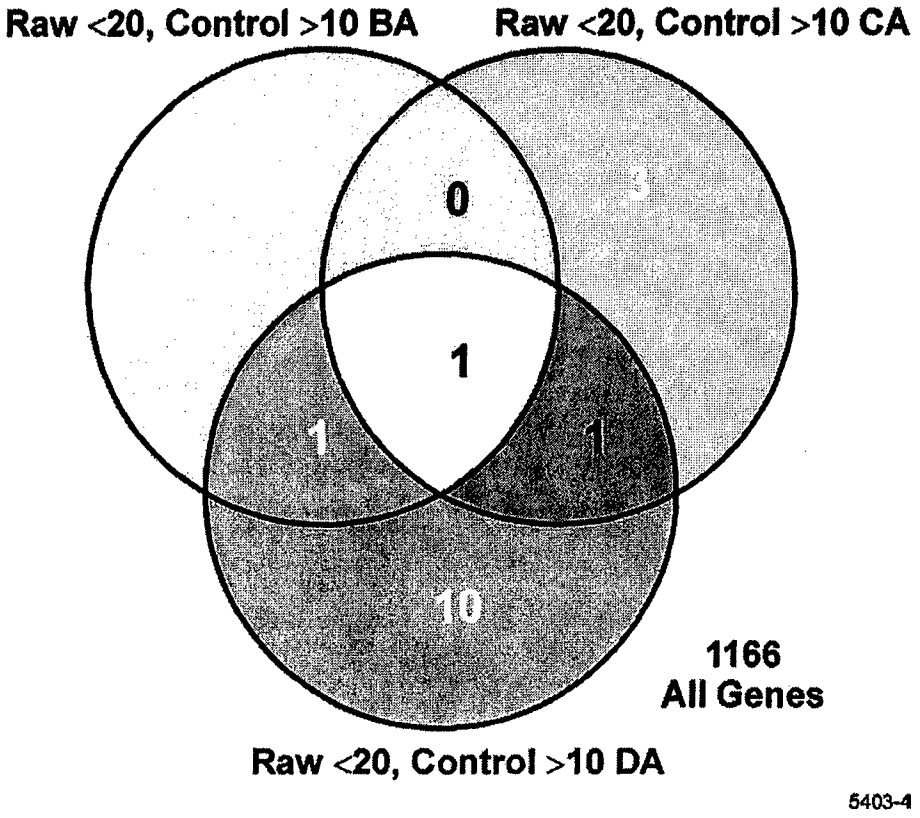

Figure 16. Venn diagram of genes expressed in muscle, but absent in tumors. (A = skeletal muscle, B = Thorotrast® fibrosarcomas, C = Thorotrast® MFH, D = DU MFH)

APPENDIX C

Diagnostic Criteria for Soft Tissue Tumors

- Benign fibrous histiocytoma (Based on Greaves, 1997)
  Fibrous mass; intercellular collagen; spindle cells in a storiform or cartwheel pattern; little or no cellular pleomorphism or mitotic activity

- Malignant fibrous histiocytoma (Based on Greaves, 1997)
  Solid fibrous mass; intercellular collagen; variable storiform pattern of plump uniform to bizarre spindle cells; pleomorphic giant cells; mitotic activity; infiltration of local tissues; occasional metastasis

- Fibroma (Based on Greaves, 1997)
  Dense fibrous mass, abundant collagenous stroma; small sparse spindle cells with small dense nuclei; few or no mitoses

- Fibrosarcoma (Based on Greaves, 1997)
  Solid fibrous mass; collagen stroma; monomorphic interwoven fascicles of plump spindle cells; herring bone pattern; mitotic activity; local invasion

- Osteosarcoma (Based on Greaves, 1997)
  Solid fibrous mass; collagen stroma; pleomorphic cells; osteoid or bone matrix; mitotic activity; local invasion

- Myoblastoma, Granular cell (Based on Enzinger and Weiss 1995)
  Cellular mass in muscle; scant stroma; large rounded cells; small nuclei, granular eosinophilic cytoplasm, PAS positive cytoplasmic granules; few or no mitoses

APPENDIX D

Characteristics of Implant-Associated Soft Tissue Tumors

Implant	Animal No.	DPI	Tumor Type	Vimentin Staining	Masson Staining	PAS Staining
DU 5 mm^2	F 081	715d	MFH in capsule wall (microscopic)	1	3	–
DU 5 mm^2	F 089	767d	MFH	3	2	–
DU 5 mm^2	L 090	611d	MFH	3	3	–
DU 5 mm^2	L 092	493d	Osteosarcoma	4	2	–
DU 5 mm^2	L 095	535d	MFH	3	2	–
DU 5 mm^2	L 099	582d	Fibrosarcoma	3	3	–
DU 5 mm^2	R 093	696d	MFH	no tissue	no tissue	no tissue
DU 5 mm^2	R 094	635d	MFH	3	4	–
DU 5 mm^2	R 100	572d	Osteosarcoma	4	4	–
DU 2.5 mm^2	E 068	515d	Benign Fib. Histiocytoma (caps.)	2	3	–
DU 2.5 mm^2	E 071	601d	Right leg - MFH	3	2	–
			Left - Fibroma w/oss. Metaplasia	no tissue	no tissue	no tissue
DU 2.5 mm^2	K 080	855d	Fibrosarcoma in capsule (microscopic)	2	2	–
Thorotrast®	C 034	792d	Fibrosarcoma	2	3	–
Thorotrast®	C 036	670d	MFH	1	2	–
Thorotrast®	C 037	562d	MFH	2	2	–
Thorotrast®	C 038	547d	Fibrosarcoma (seen @ trim)	1	2	–
Thorotrast®	C 040	728d	MFH	3	3	–
Thorotrast®	C 042	698d	MFH	2	3	–
Thorotrast®	C 045	660d	MFH	1	3	–
Thorotrast®	C 046	593d	MFH	2	1	–
Thorotrast®	C 047	799d	MFH	–	3	–
Thorotrast®	C 048	666d	Fibrosarcoma	3	4	–
Thorotrast®	I 038	645d	Osteosarcoma; Soft tissues on X-ray	2	2	2
Thorotrast®	I 041	541d	Fibrosarcoma	2	3	–
Thorotrast®	I 042	679d	MFH	2	3	–
Thorotrast®	I 043	666d	MFH	2	3	–
Thorotrast®	I 044	518d	MFH	3	3	–
Thorotrast®	I 045	586d	Fibrosarcoma	2	3	–
Thorotrast®	I 048	705d	MFH	2	-	–
Thorotrast®	I 050	621d	Fibrosarcoma	2	2	–
Thorotrast®	I 051	799d	MFH	2	3	–
Thorotrast®	O 040	714d	Fibrosarcoma in muscle	–	3	–
Thorotrast®	O 042	712d	Fibrosarcoma	3	4	–
Thorotrast®	O 044	645d	MFH in muscle	3	2	–
Thorotrast®	O 045	769d	Myoblastoma in muscle	ND	-	2
Thorotrast®	O 046	622d	Fibrosarcoma	2	3	–
Thorotrast®	O 051	607d	Fibrosarcoma (microscopic)	1	2	–
Ta 5 mm^2	H 034	592d	MFH	2	1	–
Ta 5 mm^2	N 028	987d	MFH in capsule (microscopic)	3	2	–

Staining is combined 1–4 score of intensity and distribution.

APPENDIX E

Molecular Changes in Soft Tissue Tumors

Implant	Animal No.	Tumor Type	Mets	Relation to Death	p53	MDM2	c-myc	p21	K-ras
DU 5 mm^2	F 081	MFH in capsule wall	(microscopic)	Inc	neg	neg	no tissue	neg	no tissue
DU 5 mm^2	F 089	MFH		COD	+	neg	neg	neg	no tissue
DU 5 mm^2	L 090	MFH		COD	+++	neg	neg	neg	neg
DU 5 mm^2	L 092	Osteosarcoma	Not bone	COD	neg	+	neg	+	neg
DU 5 mm^2	L 095	MFH		COD	neg	neg	neg	neg	neg
DU 5 mm^2	L 099	Fibrosarcoma	Lumbar ln	COD	neg	neg	neg	neg	neg
DU 5 mm^2	R 093	MFH		COD	neg	ND	ND	no tissue	neg
DU 5 mm^2	R 094	MFH		COD	neg	neg	neg	neg	no tissue
DU 5 mm^2	R 100	Osteosarcoma	Not bone	COD	neg	neg	neg	neg	neg
DU 2.5 mm^2	E 068	Benign Fibrous Histiocytoma in capsule		Inc	neg	neg	no tissue	no tissue	no tissue
DU 2.5 mm^2	E 071	Right leg - MFH		COD	++++	neg	neg	neg	no tissue
		Left leg - Fibroma w/osseous metaplasia		Inc	no tissue	no tissue	no tissue	no tissue	no tissue
DU 2.5 mm^2	K 080	Fibrosarcoma in capsule	(microscopic)	Inc	neg	neg	no tissue	no tissue	no tissue
Thorotrast®	C 034	Fibrosarcoma		COD	neg	neg	++	neg	neg
Thorotrast®	C 036	MFH		COD	neg	neg	neg	neg	neg
Thorotrast®	C 037	MFH		COD	neg	neg	neg	neg	neg
Thorotrast®	C 038	Fibrosarcoma	(seen @ trim)	Inc	neg	neg	neg	neg	no tissue
Thorotrast®	C 040	MFH		COD	neg	neg	neg	neg	neg
Thorotrast®	C 042	MFH		COD	neg	neg	neg	neg	neg
Thorotrast®	C 045	MFH		COD	neg	neg	neg	neg	neg
Thorotrast®	C 046	MFH		COD	neg	neg	++	neg	neg
Thorotrast®	C 047	MFH		COD	neg	neg	neg	neg	neg
Thorotrast®	C 048	Fibrosarcoma		COD	neg	neg	neg	neg	neg

Molecular Changes in Soft Tissue Tumors (Concluded)

Implant	Animal No.	Tumor Type	Mets	Relation to Death	p53	MDM2	c-myc	p21	K-ras
Thorotrast®	I 038	Osteosarcoma	Not bone; Lung	COD	neg	neg	neg	neg	neg
Thorotrast®	I 041	Fibrosarcoma		COD	neg	+	neg	+	neg
Thorotrast®	I 042	MFH		COD	neg	neg	neg	neg	neg
Thorotrast®	I 043	MFH		COD	neg	neg	neg	neg	neg
Thorotrast®	I 044	MFH		COD	neg	+	neg	+	neg
Thorotrast®	I 045	Fibrosarcoma		COD	neg	neg	neg	neg	neg
Thorotrast®	I 048	MFH		COD	neg	neg	neg	neg	neg
Thorotrast®	I 050	Fibrosarcoma		COD	neg	neg	neg	neg	neg
Thorotrast®	I 051	MFH		COD	neg	neg	neg	neg	neg
Thorotrast®	O 040	Fibrosarcoma	in muscle	Inc	neg	neg	no tissue	neg	no tissue
Thorotrast®	O 042	Fibrosarcoma		COD	neg	neg	ND	neg	neg
Thorotrast®	O 044	MFH	in muscle	Inc	neg	neg	no tissue	neg	no tissue
Thorotrast®	O 045	Myoblastoma	in muscle	Inc	neg	neg	no tissue	neg	no tissue
Thorotrast®	O 046	Fibrosarcoma		COD	neg	neg	neg	neg	neg
Thorotrast®	O 051	Fibrosarcoma	microscopic	Inc	neg	neg	no tissue	neg	no tissue
Ta 5 mm^2	H 034	MFH		COD	neg	+	+	+	neg
Ta 5 mm^2	N 028	MFH in capsule	microscopic	Inc	++	neg	no tissue	neg	no tissue
DU 2.5 mm^2	E 077	Myoblastoma	Muscle, Not assoc	Inc	neg	neg	+	neg	neg
Ta 5 mm^2	H 032	Fibrosarcoma	Muscle, Not assoc	COD	neg	neg	ND	neg	neg

APPENDIX F

Differential Gene Expression of Tumor Samples Determined with cDNA Arrays

Table F.1. Thorotrast Fibrosarcomas vs. Skeletal Muscles (BA) – Significant Increased Gene Expression ($p < 0.05$)

Systematic	Normal-ized	t-test P-value	Genbank	Description
U61261	0.62	0.005	B13g	laminin alpha 3 subunit (LAMA3)
L31883	5.28	0.006	F07f	tissue inhibitor of metalloproteinase 1 (TIMP1)
X56133	0.69	0.012	C02j	mitochondrial H+ transporting ATP synthase F1 complex alpha subunit isoform 1 (ATP5A1; ATPM)
M64797	0.56	0.021	C02b	testis fructose-6-phosphate 2-kinase/fructose 2,6-biphosphate (testis 6PF-2-K/fru-2,6-P2ase); 6-phosphofructo-2-kinase; fructose 2,6-bisphosphatase
D13376	0.39	0.025	C06h	adenylate kinase 1 (AK1); ATP/AMP transphosphorylase; myokinase
Y13380	0.29	0.028	B14d	amphiphysin II (AMPH2)
J02635	3.93	0.031	F06h	alpha-2 macroglobulin
M65253	2.35	0.032	A11d	34A transformation-associated protein; TAP-related matrix metalloproteinase 10 (MMP10); stromelysin 2 (SL2); transin 2
M15768	1.43	0.033	A01h	CD4 homologue, W3/25 antigen
X64827	0.21	0.034	C03a	cytochrome c oxidase polypeptide VIIIh (COX8H)
M95738	1.51	0.042	B10c	solute carrier family 6 member 11 (SLC6A11); gamma-amino-butyric acid transporter 3 (GABA-A transporter 3; GABT3)
AF115380	5.55	0.042	D01j	myeloid cell differentiation protein 1
X62952	13.93	0.046	F10i	vimentin (VIM)
AJ223083	2.01	0.046	F09h	retinoid X receptor gamma (RXR-gamma; RXRG)

Table F.2. Thorotrast MFH Tumors vs. Skeletal Muscle (CA) – Significant Increased Gene Expression ($p < 0.05$)

Systematic	Normal-ized	t-test P-value	Genbank	Description
X78167	2.77	0.001	C13l	(Sprague Dawley) ribosomal protein L15
AF198087	2.16	0.001	F07i	adrenal secretory serine protease
X59051	2.24	0.003	G47	40S ribosomal protein S29 (RPS29)
X87107	1.81	0.003	C14b	60S ribosomal protein L6 (RPL6)
AF140031	0.75	0.004	D13h	activin beta C
U57062	0.78	0.005	A11m	natural killer (NK) cell protease 4 (RNKP-4)
X82396	2.13	0.008	F06a	cathepsin B
X96967	3.80	0.011	F11b	profilin 1 (PFN1)
M19533	2.38	0.012	C12g	T-cell cyclophilin
X02918	1.93	0.015	C12f	protein disulphide isomerase (PDI)
X68282	1.58	0.021	C14d	ribosomal protein L13A
X12367	3.40	0.022	F07j	cellular glutathione peroxidase I (GSHPX1; GPX1)
D26564	0.65	0.022	A09f	CDC37
D26307	1.39	0.022	A05g	junD proto-oncogene
M32474	0.72	0.025	A09m	carcinoembryonic antigen-related protein CGM1
Z11932	0.64	0.029	D10h	vasopressin V2 receptor (AVPR2)
Z50051	0.62	0.030	A11g	complement component 4-binding protein alpha (C4B-binding protein alpha; C4BPA)
M86389	0.61	0.032	B03d	heat shock 27-kDa protein (HSP27)
D10554	0.61	0.032	A04l	hepatocyte nuclear factor 4 alpha (HNF4-alpha); transcription factor 14 (TCF14); nuclear receptor sub family 2 group A member 1 (NR2A1)
AJ006070	2.61	0.034	F12m	V(D)J recombination activating protein 1 (RAG1)
D00753	1.75	0.035	F06j	contrapsin-like protease inhibitor related protein; SPI-3 serine protease inhibitor
U82591	1.49	0.038	A09i	growth-related c-myc-responsive protein RCL
M58316	0.84	0.038	D04m	alpha 2C adrenergic receptor (ADRA2C); alpha 2C adrenoceptor
AB006613	6.21	0.038	F14e	mitochondrial uncoupling protein 2 (UCP2)
L08490	0.52	0.041	D11a	Gamma-aminobutyric-acid receptor alpha 1subunit (GABA[A] receptor alpha 1; GABRA1)
M65008	0.78	0.045	A07m	zinc finger transcriptional activator (NGFI-C)

Table F.3. DU MFH Tumors vs. Skeletal Muscle (DA) – Significant Increased Gene Expression ($p < 0.05$)

Systematic	Normal-ized	t-test P-value	Genbank	Description
U24175	2.00	0.003	F03n	signal transducer & regulator of transcription 5A1 (STAT5A1)
X54467	1.40	0.004	F04m	cathepsin D
M18668	0.28	0.005	C02k	creatine kinase b
U47287	0.64	0.006	D09i	prostaglandin F2 alpha receptor
X70871	0.59	0.007	A08l	G2/M-specific cyclin G (CCNG)
M32061	0.86	0.007	D04l	alpha 2B adrenergic receptor (ADRA2B); alpha 2B adrenoceptor
D43950 (human)	2.06	0.008	C12l	T-complex protein 1 epsilon subunit (TPC1-epsilon); CCT-epsilon (CCTE; CCT5) {rat homolog of human}
M00002	0.78	0.013	A12i	apolipoprotein AIV (APOA4; APOC4)
X65036	0.79	0.016	A09n	integrin alpha 7 (IGA7)
X02601	1.57	0.024	F05j	polypeptide, 53 kDa, growth factor induced
X58465	1.71	0.030	C14a	40S ribosomal protein S5 (RPS5)
J02744	0.54	0.033	B05c	glutathione S-transferase mu 3 (GSTM3); GST Yb3
X66370	1.92	0.035	C14g	ribosomal protein S9
U12428	0.56	0.040	A06l	early growth response protein 3
J03773	1.60	0.041	E13b	guanine nucleotide-binding regulatory, alpha subunit
L25527	0.80	0.043	A01j	E-selectin; endothelial leukocyte adhesion molecule 1 (ELAM1); leukocyte-endothelial Cell adhesion molecule 2 (LEMCAM2) CD62E
Y13336	2.17	0.044	C13j	defender against cell death 1 protein (DAD1)
J02592	0.28	0.048	B05f	glutathione S-transferase Yb2 subunit (GST Yb2); GST mu (GSTM2)
M63983	0.19	0.049	G15	hypoxanthine-guanine phosphoribosyltransferase (HPRT)

F.4. Significantly Expressed Genes Shared Among Categories

Systematic	Normal-ized	t-test P-value	Normal-ized	t-test P-value	Normal-ized	t-test P-value	Genbank	Description
					Shared by B/A, C/A, and D/A			
	B		**C**		**D**			
AF021343	0.634	0.045	0.654	0.029	0.459	0.018	C011	glycogenin
X62671	2.927	0.001	3.578	0.002	2.210	0.032	F04d	40S ribosomal protein S30 (RPS30); Finkel-Biskis-Reilly murine sarcoma virus ubiquitously express (FAU; FUB1)
					Shared by B/A and C/A, not D/A			
	B		**C**		**D**			
D63378	11.390	0.011	8.603	0.035	3.728	0.313	F06c	probable protein disulfide isomerase ER60; 50-kDa microsomal protein; HIP70
J02701	0.485	0.036	0.470	0.030	0.828	0.569	B12b	sodium/potassium-transporting ATPase beta 1 subunit (ATP1B1)
M17698	7.207	0.009	7.733	0.032	4.439	0.108	F14n	thymosin beta 10 (TMSB10; THYB10); PTMB10
L31884	10.295	0.014	8.800	0.021	1.917	0.499	F07g	tissue inhibitor of metalloproteinase 2 (TIMP2)
D10952; X14208	0.500	0.036	0.589	0.040	0.268	0.091	C02n	cytochrome c oxidase polypeptide Vb (COX5B)
U23407	2.002	0.007	1.721	0.029	1.855	0.084	F02m	cellular retinoic acid binding protein 2
X83537	4.837	0.037	4.150	0.030	1.923	0.237	A11k	matrix metalloproteinase 14 (MMP14); membrane-type matrix metalloproteinase 1 (MT-MMP1)
X53363	1.933	0.046	1.380	0.023	1.178	0.746	F01j	calreticulin (CALR); calregulin; calcium-binding protein 3 (CABP3); HACBP; ERP60
					Shared by B/A and D/A, not C/A			
	B		**C**		**D**			
AB004454	2.002	0.034	1.802	0.106	1.734	0.022	F031	presenilin 2 (PSEN2; PSNL2; PS2); apoptosis-linked gene 3 (ALG3); Alzheimer disease 4 homolog (AD4H)
V01218	0.061	0.027	0.090	0.052	0.032	0.033	F10d	skeletal muscle alpha-actin; alpha-actin 1 (ACTA1)
					Shared by C/A and D/A, not B/A			
	B		**C**		**D**			
D25224	2.333	0.051	2.307	0.020	1.786	0.046	C14c	laminin receptor 1
X51536	1.973	0.078	1.612	0.043	1.840	0.049	C13n	40S ribosomal protein S3 (RPS3)
M91599	0.647	0.353	0.552	0.041	0.527	0.036	D03j	fibroblast growth factor receptor 4 (FCFR4)
Y17295	1.460	0.354	2.441	0.013	1.907	0.025	C11m	thiol-specific antioxidant protein (1-Cys peroxiredoxin)
X57986	0.844	0.459	0.709	0.030	0.683	0.036	E08a	cAMP-dependent protein kinase catalytic subunit